SUPERSONIC FLOW IN A TWO-DIMENSIONAL ASYMMETRIC CHANNEL

Thesis by

Joseph N. Benezra

In Partial Fulfillment of the Requirements

For the Degree of

Aeronautical Engineer

California Institute of Technology

Pasadena, California

1949

ACKNOWLEDGMENT

The author wishes to express his appreciation to Dr. Allen E. Puckett not only for his able guidance in the course of this investigation but also in his assistance toward the development of the labor-saving techniques presented. He thanks Mr. Z. O. Bleviss for suggesting the subject to him and for his helpful counsel and encouragement and Mrs. E. Fox for typing the thesis.

TABLE OF CONTENTS

ABSTRACT

A practical method is developed whereby the flow field in a two-dimensional asymmetric channel can easily be determined employing the method of characteristics. Some insight as to the accuracy of such a graphical solution is gained by checking against a known theoretical solution. An asymmetric channel having a simple geometric form is designed for uniform exit flow. The lower wall is then shifted various distances to achieve different mean flows at the exit thus simulating the operation of a wind tunnel. The velocity and flow inclination gradients are determined in the test section. The same analysis is performed on a similar channel but with one of the geometric parameters of the throat changed. Finally, an investigation is carried out to determine the amount that the profile of the upper wall differs from what it should be to attain uniform flow in the test section for the various configurations.

FIGURE INDEX

FIGURE INDEX (Cont'd)

I. INTRODUCTION

The determination of the supersonic flow field in a two-dimensional asymmetric channel is of interest from both the academic and practical points of view. Only one major difficulty is present, however, when the method of characteristics is employed to determine the flow field. The essence of the difficulty lies in the initial construction of the field in the vicinity of the throat, i.e. in the region where the flow changes from subsonic to supersonic. Once this initial flow field has been established the field downstream may be easily constructed.

The interest in the problem from the practical point of view stems from the direct utilization of asymmetric channels in supersonic wind tunnel desigh. Just as in the case of a symmetrical channel the walls of an asymmetric channel in two dimensions may be designed so that the exit flow is uniform with a prescribed velocity. A different exit velocity can, of course, be obtained by changing the throat height and the shape of the walls to cancel all expansion waves so that the new uniform velocity obtains in the exit or test section. However, if the throat height is changed and the walls are left unaltered, manifestly the exit flow will not be uniform. It is the purpose of this investigation to ascertain the order of magnitude of the non-uniformity of the exit flow for mean exit velocities, both higher and lower than the design uniform exit velocity. Also, this investigation attempts to demonstrate the reliability of the method of characteristics itself in this particular application. Obviously, such a demonstration can be effected only by applying the characteristics method to a case where the flow is known from theoretical considerations beforehand. Such a "check" is afforded by F. Ringleb's particular solution of the hodograph equations. The

solution is worked out completely in Ref. 1.

In Ref. 2 Sauer presents a method whereby the flow field in the immediate neighborhood of the sonic line can be determined for both symmetric and asymmetric channels (profiles). Equations are presented for the dimensionless perturbation velocities for both cases. As it is desired to employ these equations as the basis for the construction of the initial flow near the throat, it is felt that the reliability of these equations should be tested at some distance away from the sonic line. Once again Ringleb's particular solution affords the means for checking the validity of these equations.

II. NOMENCLATURE

x', y'	coordinates for Ringleb flow field
x, y	coordinates at channel throat
$\tilde{u}$	x-component of velocity
$\tilde{v}$	y-component of velocity
$\tilde{w}$	resultant velocity
a	local velocity of sound
a^*	critical velocity of sound
u	$= \tilde{u}/a^* - 1$
v	$= \tilde{v}/a^*$
C_o	velocity of sound at reservoir conditions
M	Mach number
M_e	Mach number at exit
y_s	throat height
R_1	radius of curvature of lower wall for A- and B-group channels
ρ_p	radius of curvature of lower profile or streamline
ρ_s	radius of curvature of streamline
d	distance downstream of point 0.5 in. aft where upper channel wall becomes straight
A/A^*	one-dimensional area ratio
α	$= (\partial u/\partial x)_{y = 0}$
β	$= -(\partial v/\partial x)_{x = y = 0} = 1/\rho_p$
γ	ratio of specific heats, C_P/C_V
ψ	Prandtl-Meyer angle
ψ_e	Prandtl-Meyer angle at exit

θ' $= \tan^{-1} v/1+u$

θ inclination of flow relative to straight walls at exit

θ_w inclination of upper wall at throat relative to straight walls at exit

w designation of line of constant velocity, w ft./sec., in Ringleb flow field

k designation of streamline whose maximum velocity is k ft/sec. in Ringleb flow field

III. METHODS

The "method of characteristics" employed in this investigation is due to Prandtl and Busemann (Ref. 3). The particular numerical-graphical procedure used in the analyses of the various channel configurations investigated is that given by L. L. Cronvich in Ref. 4. It should be mentioned at the outset that the "lattice point" method is preferred to the "field" method of solution for two reasons: First, disturbing complications arise in the field method when the expansion waves emanating from the lower wall of an asymmetric channel strike the sonic line. Second, velocity and flow inclination gradients may be plotted and analyzed in a more straightforward manner if the flow field is known at distinct points rather than in particular areas.

A. Check on Techniques Used Against a Known Theoretical Solution

In an unpublished work Mr. Z. O. Bleviss has calculated the entire flow field of the Ringleb particular solution on the basis of Ringleb's original paper on the subject, Ref. 1. Streamlines were constructed and the flow inclination and velocity along each was carefully computed on the assumption of given reservoir conditions. Also constructed were lines of constant velocity and the variation of flow inclination along those lines was determined as well as throat positions between neighboring streamlines.

The first phase of this investigation is concerned with testing the method of characteristics itself before applying the method to more arbitrary asymmetric channels. Two streamlines are selected from the

Ringleb solution which approximate roughly the channels which are to be investigated. First to be tested is the effect of net size on the accuracy of the results. As initial points in the field two points are chosen on the constant velocity (or Mach number) line M = 1.055 as determined theoretically from Ringleb's solution. This corresponds to a net size of approximately 1.2° difference of flow inclination between the two initial points. The graphical construction of the characteristics for this case is carried out to a region just beyond the axis of symmetry of the flow field. This construction is found in the characteristic drawing No. C-1. Each time a characteristic strikes a wall (either one of the streamlines selected) the velocity at that point is determined since the inclination of flow is known along the streamlines. A somewhat finer net is used (C-2) with three initial points chosen on the M = 1.055 line. The flow inclination increment between adjacent initial points in this case is about 0.6° or approximately one-half the increment between the two initial points used for the coarser net. A comparison of the velocities at the walls, using these two net sizes, with the theoretical values is made in Fig. 1. It can be seen that some gain in accuracy is made by employing the finer net. In Tables I and II are tabulated the velocities at the various points on the walls for C-1 and C-2 respectively and their deviation from the theoretical values expressed as per cent error. In the case of C-1 the maximum error is 3% of the theoretical value but the root-mean-square error for all points along the boundaries is 1.1%. The finer net, C-2, results in a maximum error of 1% and a root-mean-square error for all boundary points of only 0.5%.

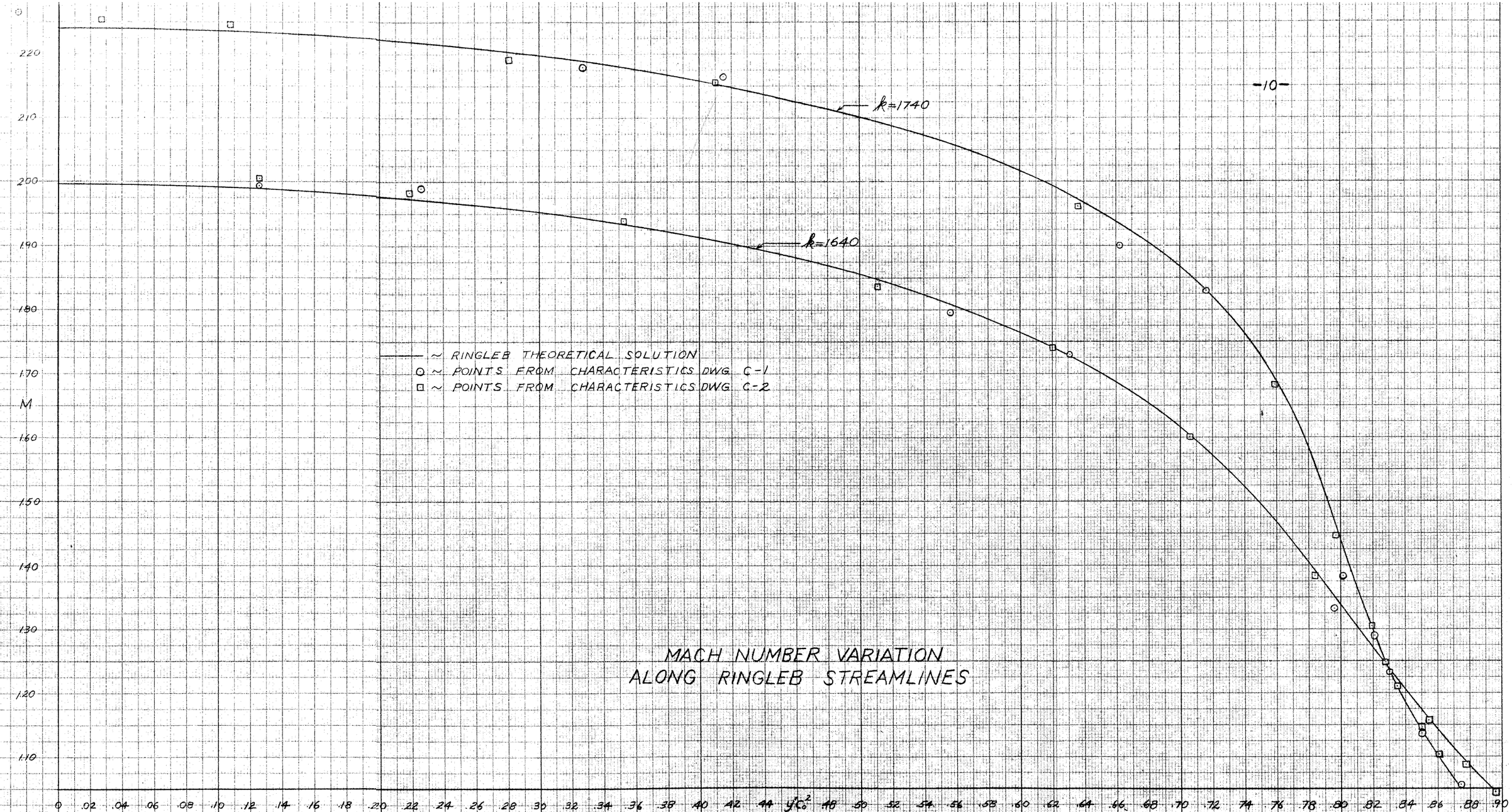

MACH NUMBER VARIATION
ALONG RINGLEB STREAMLINES

FIG. 1

FIG. 1

TABLE I - VELOCITIES ALONG RINGLEB STREAMLINES,

THEORETICAL AND GRAPHICAL--(C-1)

Pt. No.	$y'C_o^2$	M Charact. (C-1)	M Theoretical (Ringleb)	Error %
0 Initial Pt.	0.8840	1.055	1.055	---
1 Initial Pt.	.8924	1.055	1.055	---
2	.8498	1.137	1.141	-0.4
4	.8748	1.055	1.051	+0.4
5	.8210	1.290	1.290	0.0
7	.8304	1.238	1.238	0.0
8	.8015	1.334	1.425	+3.0
10	.7165	1.829	1.829	0.0
11	.7960	1.327	1.351	-1.8
13	.6626	1.901	1.934	-1.7
14	.6310	1.730	1.728	+0.1
16	.4150	2.164	2.151	+0.6
17	.5565	1.796	1.808	-0.7
19	.3276	2.179	2.190	-0.5
20	.2260	1.991	1.972	+1.0
22	-.0260	2.265	2.240	+1.1
23	.1254	1.994	1.989	+0.3

TABLE II - VELOCITIES ALONG RINGLEB STREAMLINES,

THEORETICAL AND GRAPHICAL--(C-2)

Pt. No.	$y'C_o^2$	M Charact. (C-2)	M Theoretical (Ringleb)	Error %
0 Initial Pt.	0.8789	1.055	1.055	--
3 Initial Pt.	.8924	1.055	1.055	--
4	.8611	1.103	1.099	+0.4
7	.8956	1.044	1.045	-0.1
8	.8486	1.140	1.146	-0.5
11	.8768	1.087	1.094	-0.6
15	.8546	1.156	1.160	-0.3
16	.8188	1.305	1.305	0.0
19	.8270	1.249	1.248	+0.1
20	.7968	1.446	1.460	-1.0
23	.7842	1.379	1.391	-0.9
24	.7589	1.684	1.693	-0.5
27	.7057	1.601	1.604	-0.2
28	.7096	1.844	1.845	-0.1
31	.6203	1.740	1.741	-0.1
32	.6364	1.961	1.973	-0.6
35	.5112	1.837	1.848	-0.6
36	.5179	2.094	2.088	+0.3
39	.3525	1.939	1.934	+0.2
40	.4100	2.156	2.153	+0.1
43	.2185	1.983	1.973	+0.5
44	.2814	2.192	2.203	-0.5
47	.0697	1.991	1.994	-0.2
48	.1071	2.246	2.236	+0.4
51	-.1254	2.005	1.990	+0.8
52	-.0267	2.254	2.240	+0.6

Next to be checked is the reliability of the equations Sauer gives for the perturbation velocities in a two-dimensional curved channel at some distance away from the sonic line. In Ref. 2 are found the following expressions for these perturbation velocities in an asymmetric (curved) channel:

$$u = \alpha x - \beta y + \left(\frac{\gamma+1}{2}\alpha^2 + \beta^2\right)y^2 + \cdots\cdots$$
$$v = -\beta x + \left[(\gamma+1)\alpha^2 + 2\beta^2\right]xy - \left[\frac{\gamma+1}{2}\alpha\beta + 4\beta\left(\frac{\gamma+1}{2}\alpha^2 + \beta^2\right)x\right]y^2 + \cdots \quad (1)$$

where α signifies the velocity increase, $\partial u/\partial x$, along the profile on transit through the critical velocity and,

$$\frac{1}{\rho_P} = -\left(\frac{\partial v}{\partial x}\right)_{x=y=0} = \beta \,. \quad (2)$$

Also derived are the approximate relationships

$$\frac{1}{\rho_S} \doteq \beta - \left[(\gamma+1)\alpha^2 + \beta^2\right] y_s \quad (3)$$

$$\frac{1}{\rho_S} \doteq \frac{1}{\rho_P} - \left[(\gamma+1)\alpha^2 + \frac{1}{\rho_P^2}\right] y_s \,. \quad (3a)$$

The configuration for the curved channel and orientation of axes is as shown in Fig. 2.

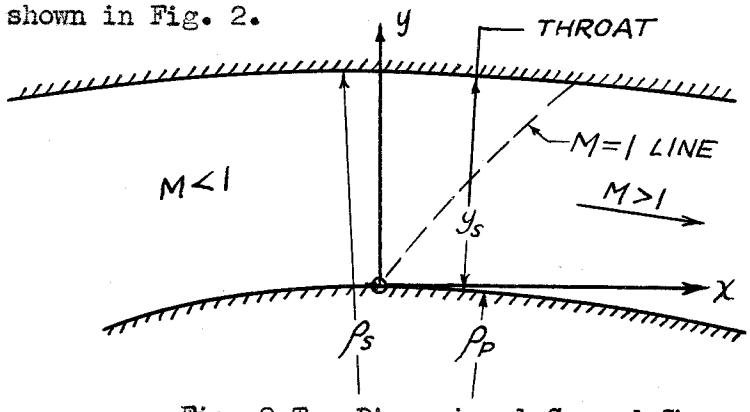

Fig. 2 Two-Dimensional Curved Channel.

Also presented in Ref. 2 are the following equations for the perturbation velocities in a two-dimensional symmetric channel:

$$u = \alpha x + \frac{\gamma+1}{2}\alpha^2 y^2 + \cdots$$
$$v = (\gamma+1)\alpha^2 x y + \frac{(\gamma+1)^2}{6}\alpha^3 y^3 + \cdots \qquad (4)$$

The following expression is also derived:

$$\frac{1}{\rho_s} = (\gamma+1)\alpha^2 y_s \,. \qquad (5)$$

The configuration for the symmetric channel and the orientation of axes is as shown in Fig. 3.

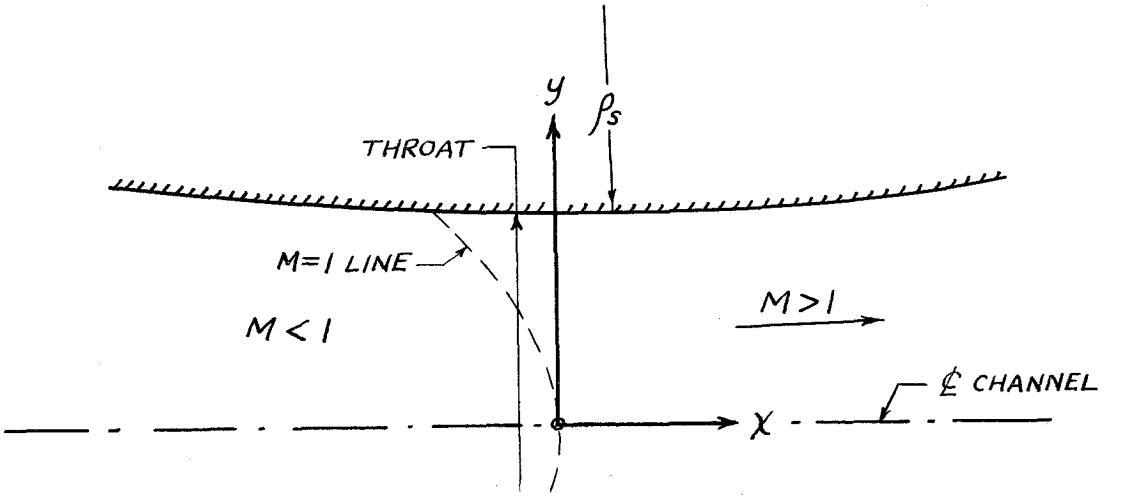

Fig. 3. Two-Dimensional Symmetric Channel

Equations (4) are obviously a limiting case of equations (1), since as $\rho_p \to \infty$ from equation (2) it is seen that $\beta \to 0$ and the expressions for u and v become identical.

On the two Ringleb streamlines already selected, k = 1640 and k = 1740, coordinate axes are erected in a manner consistent with the derivation of equations (4). The location of the axes is determined essentially by the narrowest part of the channel i.e. the geometric throat. Through the intersection of the M = 1.055 line with the streamline k = 1640, the line AA' is drawn parallel to the y axis, see Fig. 4. At the points of intersection of AA' with constant velocity lines the velocities are computed according to equations (4). The flow inclination is computed also at the intersection of AA' with the two streamlines using equations (4). Obviously, the results of these computations depend upon the radii of curvature used in determining α. As the radii of curvature change along the streamlines the values of the curvature actually used represent a mean between the curvatures at C and D for k = 1740 and a mean between those at F and E for k = 1640. In Table III are tabulated the perturbation velocities, Mach numbers and flow inclinations both as obtained theoretically and also using equations (4), and the per cent and absolute error between the last two quantities.

With errors in velocity of the order of 2 per cent and flow inclination of 0.2° to 1.0° it is conceivable that the use of equations (4) and the more general equations (1) might be seriously limited. To verify this the entire flow field between the two streamlines is constructed (C-3) using six initial points equally spaced on AA', the end points lying on the streamlines. The velocity and flow inclination* at each initial point are determined from equations (4). The difference in flow inclination and Prandtl-Meyer angle between adjacent points on the

*The flow inclination assigned to each point is done by a scheme of pro-rating described in the Appendix.

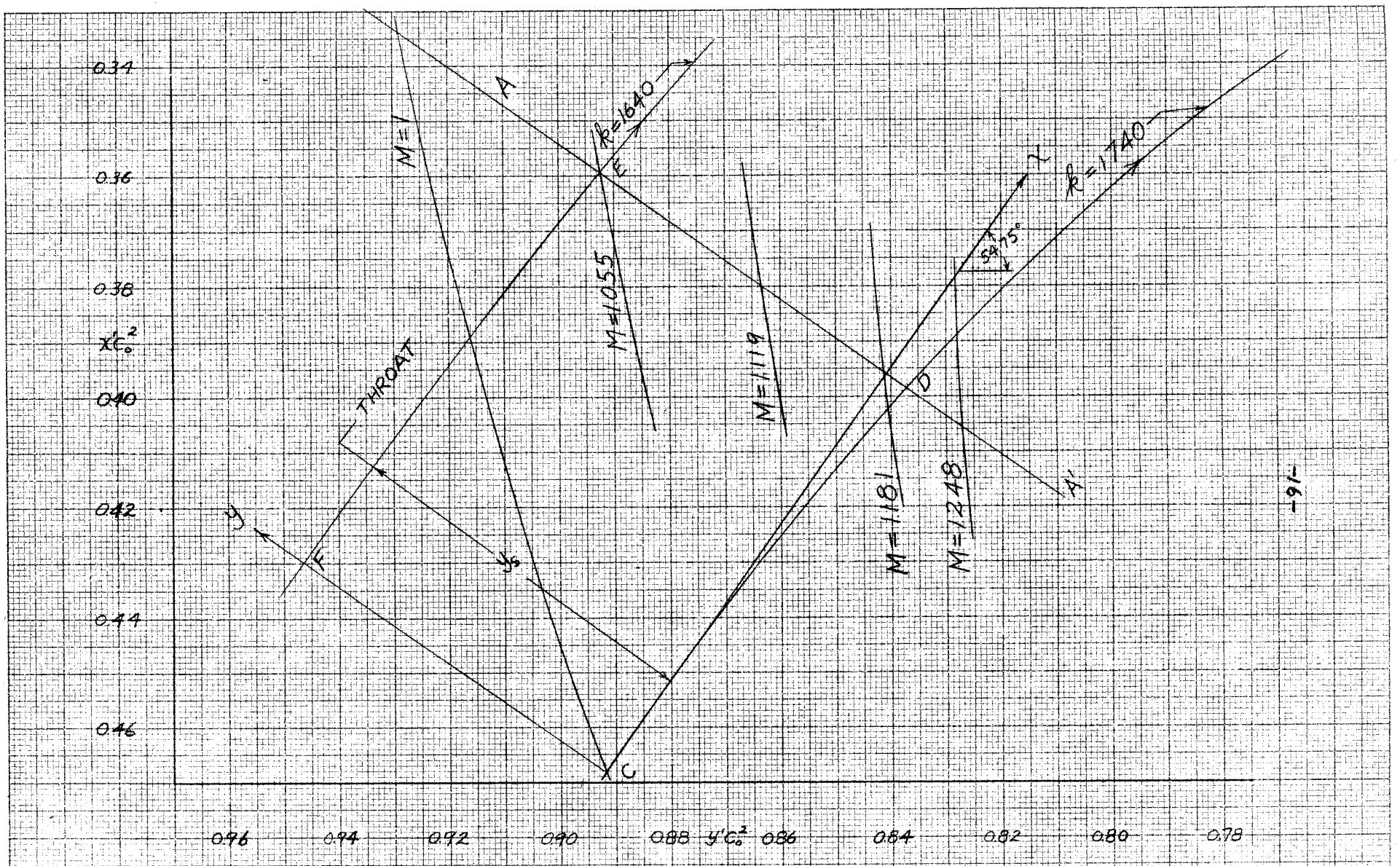

THROAT REGION BETWEEN RINGLEB STREAMLINES

FIG 4

TABLE III - VELOCITIES AND FLOW INCLINATIONS, THEORETICAL

AND THOSE GIVEN BY EQ'S. (4),

ALONG A CERTAIN LINE IN THE RINGLEB FLOW FIELD.

x	y	u	v	$\tilde{w}/a^*$	M Eq's.(4) (Sauer)	M Theoretical (Ringleb)	Percent Error in M	54.75+ θ' (Sauer)	θ (Ringleb)	54.75+ θ'-θ
			$\rho_s = 1.20$; $\rho_p = 0.80$ (Mean Values)							
0.0885	0.1084	0.0347	-0.0803	1.037	1.045	1.000	4.50			
↓	.0634	.0608	-.0810	1.064	1.078	1.055	2.18	50.37°	50.2°	.17°
	.0279	.0924	-.0940	1.097	1.120	1.119	0.09			
	.0007	.1233	-.1101	1.130	1.163	1.181	-1.52			
	-.0042	.1295	-.1136	1.136	1.170	1.199	-2.42	49.01	48.0	1.01
	-.0168	.1463	-.1234	1.152	1.191	1.248	-4.57			

-17-

initial line AA' varies but is of the order of 0.4°.

Velocity gradients at stations a, b, and c (see Fig. 5) are compared with the theoretical values in Figures 6, 7, and 8, and tabulated in Table IV are both the velocities as obtained by characteristics (C-3) along the two streamlines and the corresponding theoretical values together with the per cent error. One of the streamlines between the two selected is drawn in C-3, viz. $k = 1700$. The flow inclinations along this streamline as obtained by the method of characteristics are compared with the theoretical values in Fig. 9. The agreement of both velocities at the three stations and flow inclination along $k = 1700$ with the theoretical values are seen to be excellent. The maximum error in velocity is 0.5% and error in flow inclination is 0.3°. Along the channel boundaries beyond the point about midway between throat and exit (axis of flow field symmetry) the maximum error in velocity is 0.6% and the root-mean-square error is only 0.3%. These errors are less than the corresponding errors obtained from either C-1 or C-2 where exact initial data is used. The superior accuracy is due to the finer net employed. The agreement is even more remarkable inasmuch as simple linear interpolation is employed here (and in the other channels investigated) to ascertain values of velocity and flow inclination on the characteristic lines between lattice points. It should be remembered that, contrary to what is expected, the agreement is very good in spite of the serious errors in velocity and flow inclination at the initial points from which the solution by characteristics is carried out. Therefore, it is concluded that the initial distribution of velocity and flow inclination near the throat is not critical as regards the accuracy of the flow field construction at some distance downstream. In other words, errors in the

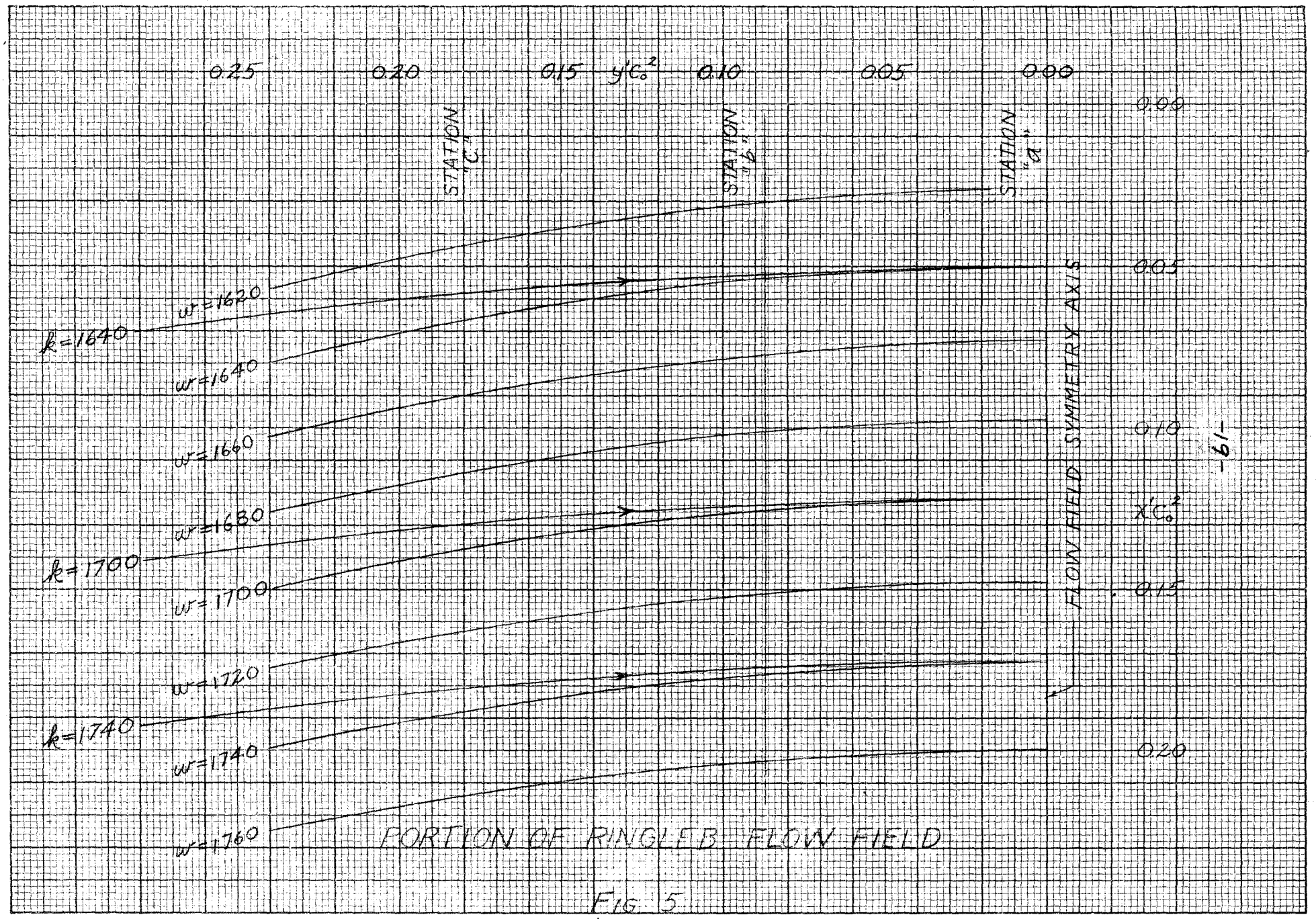

PORTION OF RINGLEB FLOW FIELD

FIG. 5

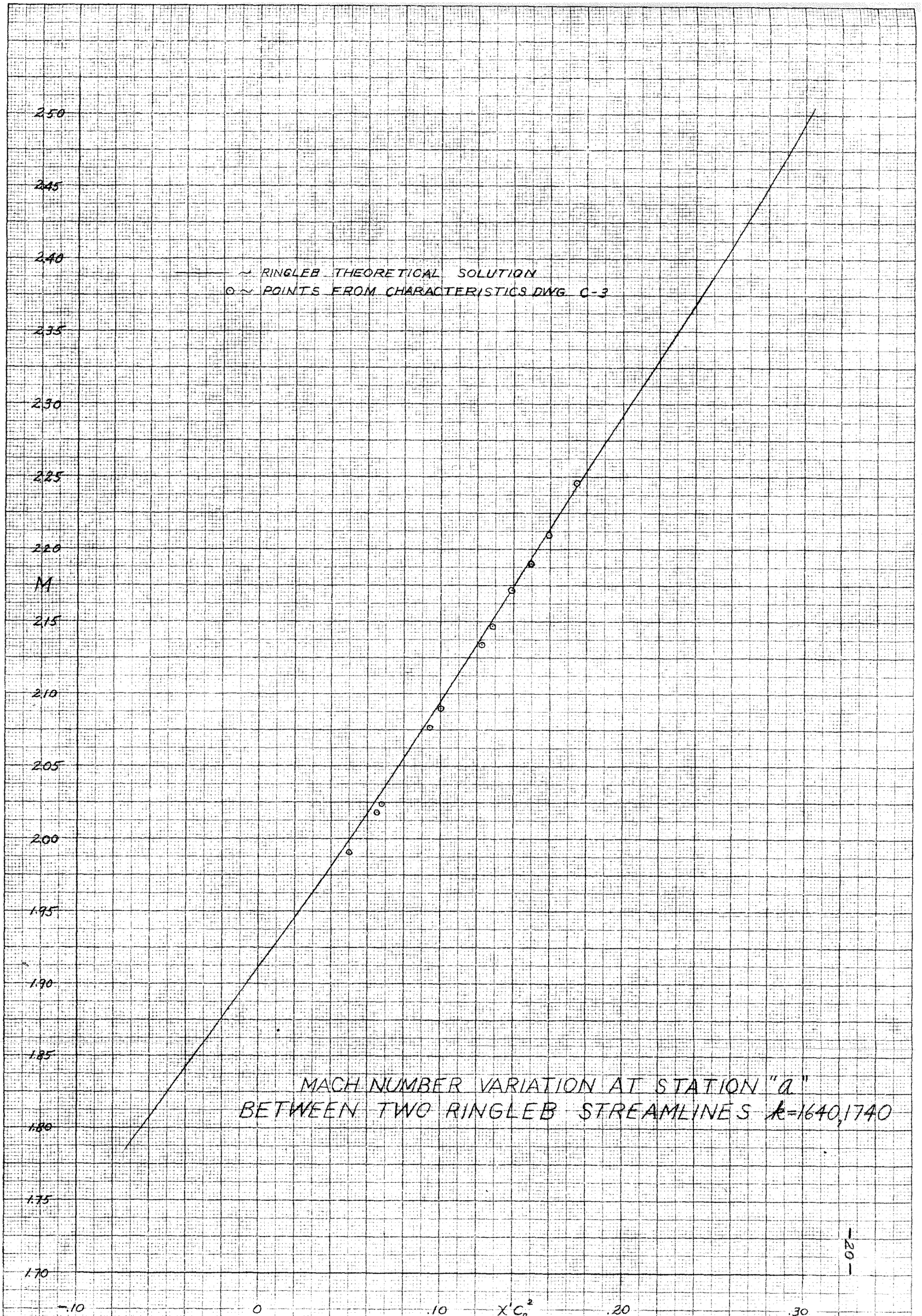
2.50
2.45
2.40
2.35
2.30
2.25
2.20
M
2.15
2.10
2.05
2.00
1.95
1.90
1.85
1.80
1.75
1.70
—— ~ RINGLEB THEORETICAL SOLUTION
⊙ ~ POINTS FROM CHARACTERISTICS DWG C-3
MACH NUMBER VARIATION AT STATION "a"
BETWEEN TWO RINGLEB STREAMLINES k=1640,1740
-.10
0
.10
X'C₀²
.20
.30
120

FIG. 6

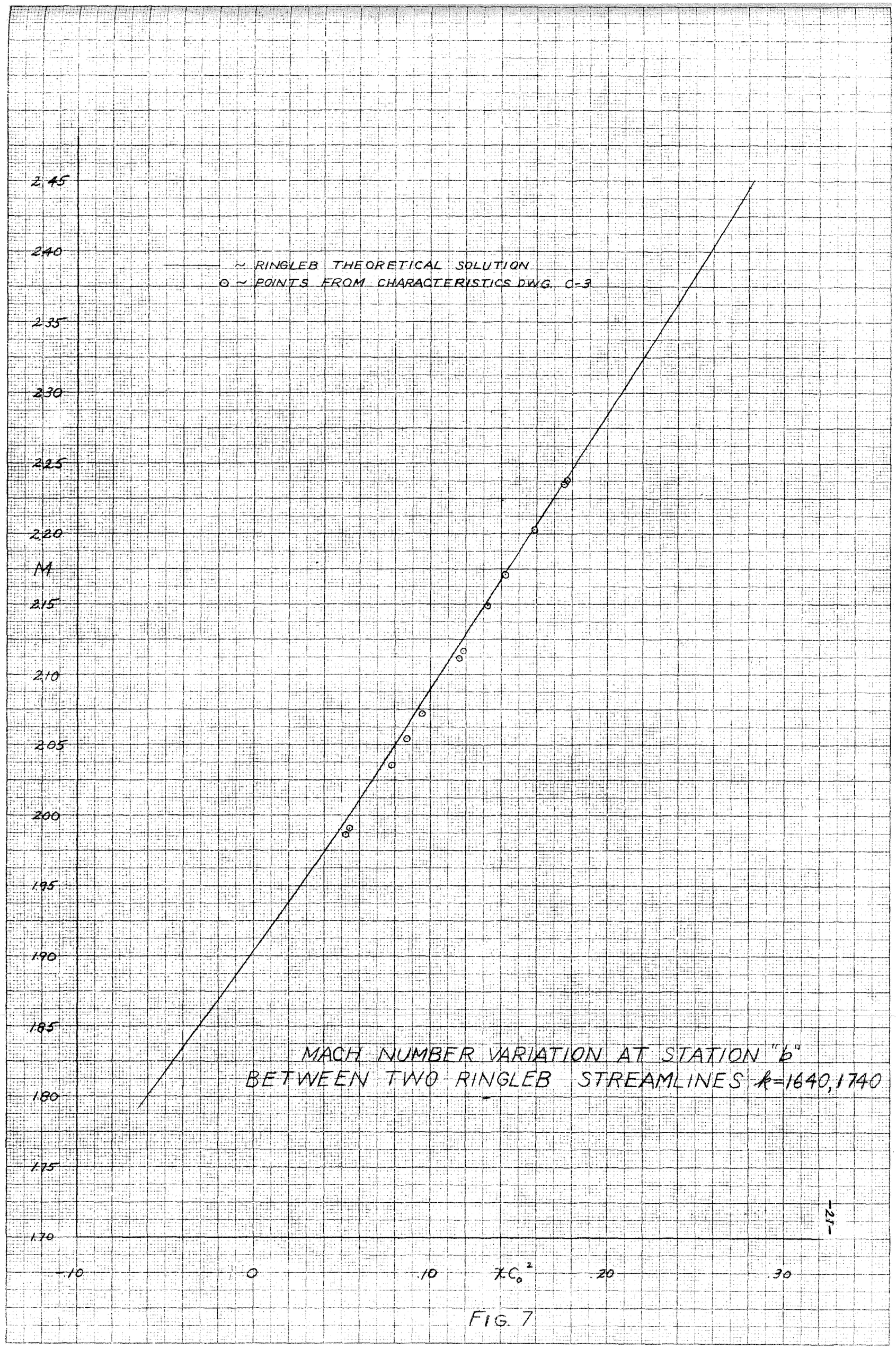

MACH NUMBER VARIATION AT STATION "b"
BETWEEN TWO RINGLEB STREAMLINES k=1640, 1740

FIG. 7

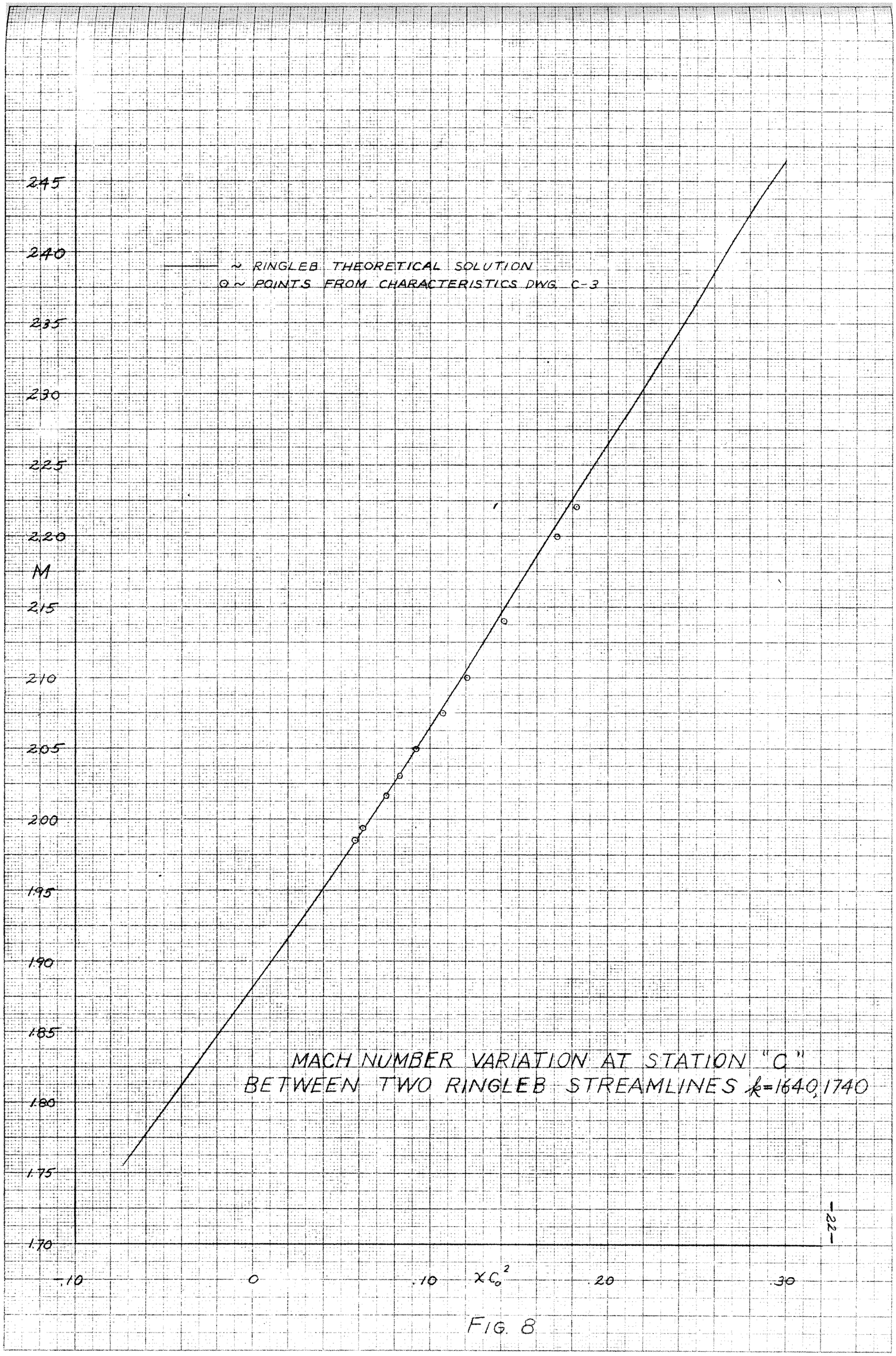

MACH NUMBER VARIATION AT STATION "C"
BETWEEN TWO RINGLEB STREAMLINES k=1640, 1740

FIG. 8

TABLE IV - VELOCITIES ALONG RINGLEB STREAMLINES,

THEORETICAL AND GRAPHICAL--(C-3)

Pt. No.	$y'C_o^2$	M Charact. (C-3)	M Theoretical (Ringleb)	Error %
0 Initial Pt.	.8367	1.170	1.199	-2.4
5 " "	.8924	1.078	1.055	+2.2
121	0.7504	1.717	1.727	-0.6
126	.8064	1.327	1.316	+0.7
187	.6480	1.954	1.956	-0.1
192	.6660	1.673	1.677	-0.2
264	.4015	2.160	2.158	+0.1
269	.4286	1.891	1.889	+0.1
275	.3690	2.176	2.173	+0.1
280	.3915	1.914	1.918	-0.2
286	.3393	2.186	2.185	0.0
291	.3312	1.944	1.942	+0.1
297	.3017	2.184	2.197	-0.6
302	.2910	1.957	1.957	0.0
308	.2460	2.204	2.214	-0.4
313	.2377	1.979	1.969	+0.5
319	.1936	2.211	2.224	-0.6
324	.2065	1.979	1.977	+0.1
330	.1530	2.231	2.230	+0.0
335	.1668	1.987	1.983	+0.2
341	.0907	2.238	2.237	0.0
346	.1335	1.987	1.988	0.0
352	.0503	2.242	2.239	+0.1
357	.0910	1.987	1.992	-0.3
363	-.0020	2.246	2.241	+0.2
368	.0265	1.991	1.995	-0.2
374	-.0312	2.238	2.240	+0.1
379	-.0317	1.991	1.995	-0.2

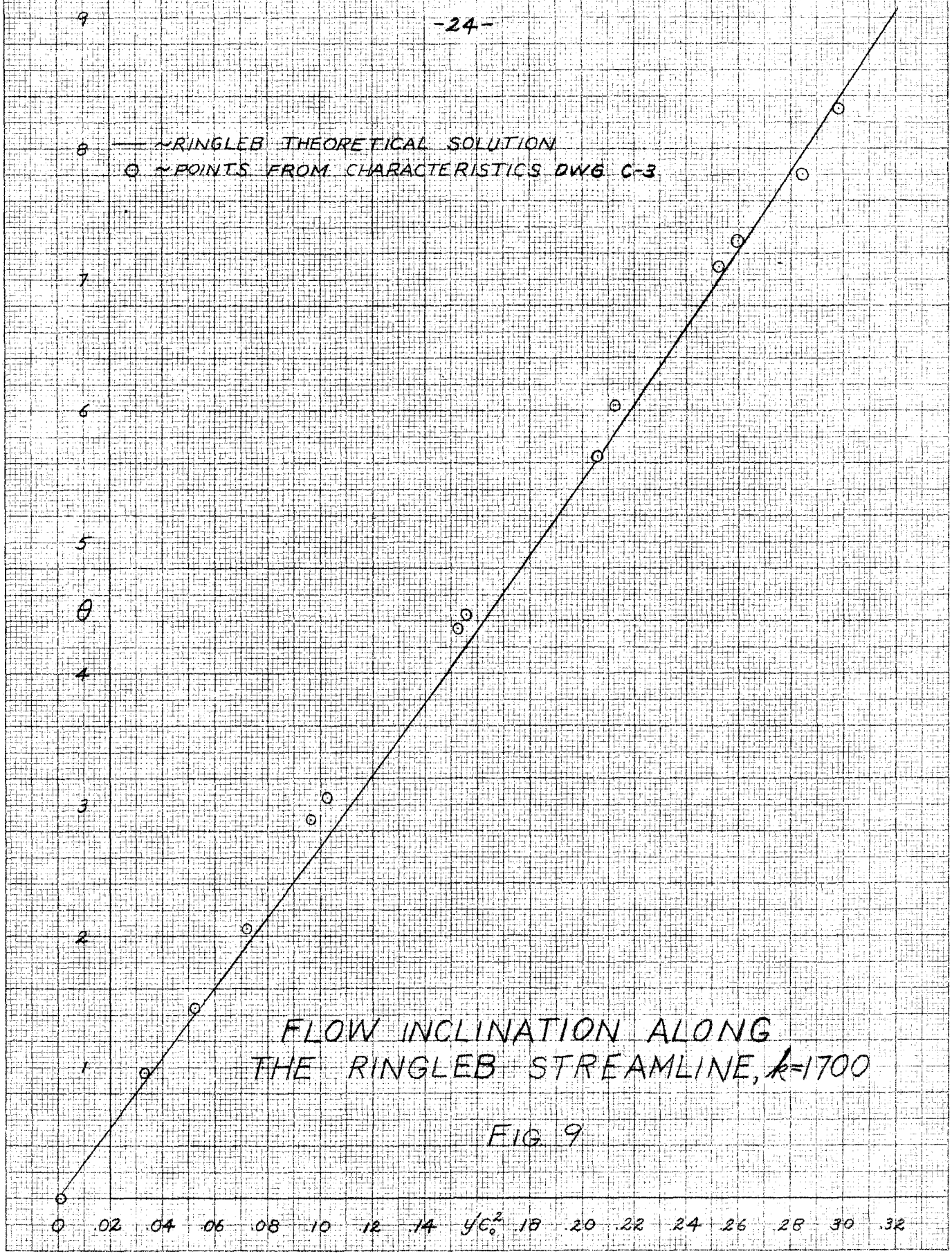

FLOW INCLINATION ALONG THE RINGLEB STREAMLINE, k=1700

FIG. 9

distribution of velocity and flow inclination along the initial line near the throat "wash out" downstream.

B. Simplification of the Initial Flow Field

Since the method of characteristics requires that a pair of simultaneous linear algebraic equations be solved in order to determine the velocity and flow inclination at each new lattice point, it is immediately apparent that the labor involved becomes great as finer nets are used and many channels are investigated. The fact of the relative insensitivity of the flow field some distance downstream of the throat to the initial values of velocity and flow inclination assumed in that region affords the following simplification in the technique used for the construction of the flow field in the two-dimensional channels to be investigated presently thus greatly reducing the labor of computation. The distribution of velocity and flow inclination is modified in such a manner that conditions at new lattice points can be determined simply by inspection. The method may be explained as follows:

Consider the points for which the velocity and flow inclination are known on some line within the flow field. Let ψ_i and θ_i represent the Prandtl-Meyer angle and the flow inclination with respect to a datum line. Since $\theta - \psi$ is constant along characteristics of the lower family, i.e. characteristics which run from left to right from the lower wall when the flow is from left to right, and $\theta + \psi$ is constant along characteristics of the upper family, we have for the unknown values at points 4 and 5, referring to Fig. 10, when the data at points 1, 2, 3

are known

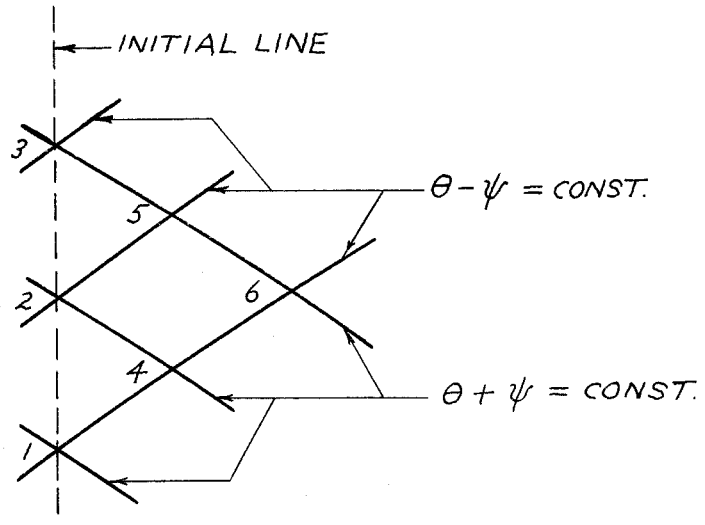

Fig. 10. Characteristics Net

$$\theta_4 = \frac{\theta_1+\theta_2}{2} + \frac{\psi_2-\psi_1}{2}$$

or

$$\theta_4 = \theta_1 + \frac{\Delta\theta_{2-1}}{2} + \frac{\Delta\psi_{2-1}}{2} ,$$

and

$$\psi_4 = \frac{\psi_1+\psi_2}{2} + \frac{\theta_2-\theta_1}{2}$$

or

$$\psi_4 = \psi_1 + \frac{\Delta\psi_{2-1}}{2} + \frac{\Delta\theta_{2-1}}{2} ,$$

where

$$\Delta\theta_{2-1} = \frac{\theta_2-\theta_1}{2}, \quad \Delta\psi_{2-1} = \frac{\psi_2-\psi_1}{2} ;$$

similarly,

$$\theta_5 = \theta_2 + \frac{\Delta\theta_{3-2}}{2} + \frac{\Delta\psi_{3-2}}{2}$$

$$\psi_5 = \psi_2 + \frac{\Delta\psi_{3-2}}{2} + \frac{\Delta\theta_{3-2}}{2} .$$

Now, if it is prescribed that

$$\Delta\theta_{2-1} = \Delta\theta_{3-2} = \cdots\cdots = \Delta\theta_{n-(n-1)} = -\Delta\psi_{2-1} = -\Delta\psi_{3-2} = \cdots\cdots = -\Delta\psi_{n-(n-1)}$$

along the initial line on which lie the points 1, 2, 3, etc., i.e. if along the initial line

$$\frac{d\psi}{d\theta} = -1 \quad ^{*},$$

then it follows

$$\psi_1 = \psi_4 = \psi_6 = \cdots \text{etc}; \qquad \theta_1 = \theta_4 = \theta_6 = \cdots \text{etc.}$$

$$\psi_2 = \psi_5 = \cdots \text{etc}; \qquad \theta_2 = \theta_5 = \cdots \text{etc.}$$

Thus, this is equivalent to prescribing Prandtl-Meyer flow (simple wave) in the region concerned since the velocity and flow inclination are constant along one family of characteristics. This is an ideal condition which obtains only approximately in the channels that are investigated. In the channels of the type investigated the region where Prandtl-Meyer flow is assumed is shown in the shaded area ABC of Fig. 11 where AC forms part of the characteristic of the lower family emanating from the point A

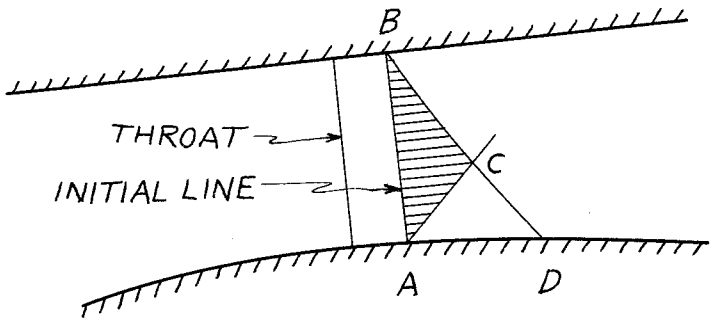

Fig. 11. Region of Assumed Prandtl-Meyer Flow in an Asymmetric Channel

*The right-hand side of this equation may be 1; however, -1 is consistent with the sign convention adopted for θ in the channels to be investigated.

on the lower wall and BC forms part of the characteristic of the upper family emanating from point B on the upper wall. The line AB is the initial line on which the flow data is prescribed. Upon investigating the flow from A to D along the lower wall using equations (4) of several different channel configurations, it turns out that $\frac{d\psi}{d\theta}$ is approximately equal to -1 along that portion of the wall. Consequently, in the whole triangular region ABD is assumed the existence of Prandtl-Meyer flow.

The construction of the remainder of the flow field downstream of the characteristic BD is then a simple matter using a computing form such as that outlined in Ref. 4. Owing to the assumption of the simplified flow in ABD the data at each new lattice point can be written down immediately by inspection. In Fig. 26 the entire graphical construction is shown for one particular channel configuration (A-3) with the values of θ and ψ written at each lattice point.

In the technique just described it is not specified how the values of ψ and θ are to be assigned to the points on the initial line. Obviously there are an infinite number of sets of values which will satisfy the relationship $\frac{d\psi}{d\theta} = -1$ on that line; however, equations (4) for the perturbation velocities are used as a guide. The procedure is as follows:

Coordinate axes for each channel are erected in a manner consistent with equations (4). Although asymmetric channels only are investigated, the geometry assumed in the throat region (to be described below) warrants the use of equations (4) rather than the less simple equations (1).

The initial line may be straight or curved and lie anywhere in the supersonic zone so long as it does not coincide with or is tangent to a characteristic in the field. For simplicity the initial line is chosen straight and parallel to the y axis and intersecting the upper wall at the point where M = 1.050* as computed from equation (4) (see Fig. 1-a in the Appendix.) Several points are chosen at equal space intervals on the initial line with the two end points lying on the walls. The number of points so selected depends upon the fineness of the net, hence on the accuracy desired. The velocity (Mach number) and flow inclination is computed at each of the points and the Prandtl-Meyer angle, ψ, corresponding to the velocity at each point is plotted against the corresponding flow inclinations. One of these plots for a typical channel, A-3, is found in Fig. 2-a of the Appendix with the relevant calculations immediately preceding that figure.

The object now is to replace the actual ψ variation with θ by a variation such that the relationship $\frac{d\psi}{d\theta} = -1$ obtains along the initial line and the increments of θ and ψ are the same between any two adjacent points. Such a curve is shown in Fig. 2d on which the position of the initial points is indicated; the curve is necessarily a straight line. Clearly, the positions of corresponding initial points on the two curves are appreciably different. However, it should be borne in mind that the exit flow is relatively insensitive to the velocity and flow inclination distribution assumed along the initial line providing it is not too distant from the sonic line. The actual straight line chosen may be displaced up or down and right or left, within limits, without affecting the qualatative results to be

*This point need not be located where M = 1.050; it is necessary only that it be in a slightly supersonic field so that the characteristics will be inclined away from the initial line.

obtained. To justify further the use of this simplification two channels are drawn for uniform exit flow: one utilizing the simplification described above, A-1, the other utilizing equations (4) to describe the velocity and flow inclination distribution along the initial line, A-2. The upper walls in both cases, which are the only part of the channels which effect the cancellation of waves, are practically coincident. The lack of coincidence is due primarily to an inherent characteristic of the lattice point method, viz. the exit Mach number cannot in general be duplicated or prescribed exactly owing to the fact that the cancellation of the waves must be commenc ed at a value of $\theta + \psi$ on the upper wall equal or very nearly equal to the Prandtl-Meyer angle at the exit, ψ_e, which it is desired to match. The quantity $\theta + \psi$ will assume certain values at definite points where the characteristics of the lower family impinge upon the upper wall. Cancellation of waves must be commenced at a point on the wall at which the value of $\theta + \psi$ is closest to the value of ψ_e that is desired. The manner by which the upper wall is designed to effect cancellation of waves is described in the Appendix.

IV. GEOMETRIC FORM OF ASYMMETRIC CHANNELS

Evidently any number of channels with different geometric parameters may be investigated by systematically varying one parameter at a time. To simplify this aspect of the problem the number of parameters is reduced to three: (1) the initial inclination of the channel, θ_w, with respect to the direction of flow at the exit, (2) the exit Mach number, or its equivalent -- the ratio of exit height to throat height, and (3) the ratio of the radius of curvature of the lower wall to the throat height. Further simplifications in the geometry are made by constructing the lower wall as a circular arc tangent to a straight line and the upper wall as a straight line up to a point where expansion waves from the lower wall are cancelled out. At the exit the upper wall is parallel to the lower. These geometric features are seen in Fig. 26. The mean exit Mach number can be changed by varying the ratio of the exit area to the throat area. In the application of this arrangement to supersonic wind tunnel design the exit or test section must be of uniform height (neglecting the effect of boundary layer growth) for all mean velocities in the test section. The area ratio can be changed by sliding one wall relative to the other in a direction parallel or normal to the test section walls. Since the former method is the one actually used in wind tunnel design, the area ratios of these channels are also altered in this manner.

In Table V are tabulated all the flow characteristic drawings of the Ringleb channel (streamlines) and the more arbitrary channels. Only one of the parameters viz. the initial channel inclination, θ_w,

TABLE V - CHARACTERISTICS DRAWING SUMMARY

Charact. Dwg. No.	Flow Field Near Throat	Throat Height, y_s	No. of Pts. on Initial Line	R_1	R_1/y_s	ρ_s/y_s	θ_w	$\Delta\psi$	A_e	Flow Field at Exit	A_e/y_s	Shift of Lower Wall	M_e (Mean)	A/A^*	% Error in Area Ratio
C-1	Theo-retical	2.61"	2	--	--	--	--	0	4.91"	Non-uni-form	1.88	--	1.997 to 2.241		
C-2	(Ringleb)	2.61	3	--	--	--	--	0	4.91		1.88	--			
C-3	(Sauer) (Eqs.4)	2.61	6	--	--	--	--	Varies	4.91		1.88	--			
A-1	P-M	4.00	7	20"	5	∞	30°	.5°	8.59"	Unif.	2.15	0"	2.297 (Design)	2.187	-1.7
A-2	Sauer	4.00	6	20	5			Varies	8.60	Unif.	2.15	0	2.293 (Design)	2.179	-1.3
A-3	P-M	3.28	7	20	6.1			.4	8.59	Non-Unif.	2.62	-1.40	2.51	2.67	-1.9
A-4	P-M	4.70	7	20	4.26			.6	8.59	Non-Unif.	1.83	1.42	2.12	1.87	-2.1
A-5	P-M	5.98	7	20	3.34			.5	8.59	Non-Unif.	1.44	3.98	1.83	1.47	-2.0
A-6	P-M	5.90	7	20	3.39			.4	8.78	Unif.	1.49	3.86	1.865 (Design)	1.513	-1.6
B-1	P-M	4.00	7	20	5		45°	.5	16.25	Unif.	4.06	0	2.973 (Design)	4.127	-1.6
B-2	P-M	3.28	7	20	6.1			.4		Non-Unif.	4.95	-.99	3.17	4.98	-.6

TABLE V (Cont'd)

Charact. Dwg. No.	Flow Field Near Throat	Throat Height, y_s	No. of Pts. on Initial Line	R_1	R_1/y_s	ρ_s/y_s	θ_w	$\Delta\psi$	A_e	Flow Field at Exit	A_e/y_s	Shift of Lower Wall	M_e (Mean)	A/A^*	% Error in Area Ratio
B-3*	P-M	3.28	7	20	6.1	∞	45°	.4	16.25	Non-Unif.	4.95	-.99	3.17	4.98	-.6
B-4	P-M	4.77	7	20	4.19	↓	↓	.6	↓	Non-Unif.	3.41	1.11	2.78	3.43	-.6
B-5	P-M	6.32	7	20	3.16	↓	↓	.6	↓	Non-Unif.	2.57	3.28	2.48	2.59	-.8

*Characteristics "averaged" in the more rigorous manner.

is changed from 30° in the A-group to 45° in the B-group of flow characteristic drawings. In each group the channel for uniform exit flow is constructed first. The simple one-dimensional area-velocity relationship provides the means for estimating the approximate distance it is necessary to shift the lower wall to attain different mean velocities in the test section. Investigated are velocity and flow inclination gradients in the test section for mean values of Mach number approximately 0.2 above and below and0.5 below the design values. Tabulated in Table V are also values of $\frac{Ae}{y_s}$ for each channel and the one-dimensional A/A* values for the corresponding mean exit Mach numbers; the per cent error between these two sets of numbers is also tabulated. In every case the $\frac{Ae}{y_s}$ is a little lower than the corresponding A/A* value owing to the fact that y_s is larger than A* for the equivalent one-dimensional channel. Mass flow considerations for the A-1 channel, for example, give an A* of 3.97 inches whence the area ratio becomes 2.16 which is closer to the one-dimensional area ratio. The remaining error is, of course, due to all the approximations made and to drafting inaccuracies. Gradients are investigated in that portion of the channel of about $1\frac{1}{2}$ to $2\frac{1}{2}$ test-section-height lengths beyond the point where the upper wall becomes parallel to the lower.

All drawings are made with a drafting machine with which angles can be drawn to the nearest 5 minutes. The functions of expanding flow used are from Ref. 5.

V. RESULTS OBTAINED

A. Gradients

Gradients of velocity and flow inclination in the test section are investigated for two groups of channels: (1) the A-group ($\theta = 30^{\circ}$) for which the "design" Mach number, $M = 2.297$, and off-design Mach numbers, $M \doteq 1.83$, 2.12, and 2.51, and (2) the B-group ($\theta = 45^{\circ}$) for which the "design" Mach number, $M = 2.973$, and off-design Mach numbers, $M \doteq 2.48$, 2.78 and 3.17. It should be emphasized that all the results of this investigation pertaining to gradients are obtained by simple linear interpolation between lattice points. Moreover, the characteristics are drawn from known points with slopes given by data at those points rather than with slopes given by average values at intermediate points with an iterative procedure employed at the walls. Though the latter method is more rigorous it is not used because the computations are doubled. The quantitative results would be somewhat different had the more rigorous procedure been followed, but the trends and orders of magnitude of the gradients remain essentially unchanged. This fact is actually borne out by constructing the flow field in one of the channels, B-3, beyond the region where the curvature of the characteristics becomes pronounced, and comparing the gradients so obtained with those in the same channel but with the characteristics drawn in the unaveraged manner, B-2. These comparisons appear for flow inclination gradients in Fig. 19 and for horizontal and vertical Mach number gradients in Figures 20 and 23.

Gradients of flow inclination are shown for the A-group of channels ($\theta_w = 30^o$) in Fig. 12. All flow inclinations are measured along a line midway between the two walls, i.e. the centerline of the test section. The angle of flow in the region investigated varies from $+.8^o$ to $-.8^o$ for A-5 in which the mean exit Mach number is approximately 1.83, i.e. 0.5 below the design value of 2.297. The variations are somewhat less in A-3 and A-4 for which the mean exit Mach numbers differ by ± 0.2 from the design value.

Horizontal Mach number gradients for the A-group of channels are shown in Figures 13-15 for the three mean exit Mach numbers. The gradients along the centerline are smallest within the investigated region with a maximum deviation from the mean exit velocities of 0.8 to 1.2%. At the two walls the gradients are more severe with a maximum deviation of 2.4 to 4.0%.

Vertical Mach number gradients are measured at stations 0.5, 6.5, and 12.5 inches downstream of the point where the upper wall becomes straight and parallel to the lower. The distance between stations is 0.7 the test section height. Gradients at the three stations are shown in Figures 16-18, for the three mean exit Mach numbers. It is also apparent from these figures that the velocity deviations are greatest at the walls. They also show that the velocity variations from wall to wall at the different stations change in a consistent manner with respect to the three mean exit velocities.

Flow inclination gradients are shown for the B-group of channels

($\theta_w = 45^\circ$) in Fig. 19. The magnitude of the flow inclinations along the test section centerline varies from $+1.5^\circ$ to -1.2° in the region investigated, or approximately twice the magnitudes but of the same general form as that existing for the corresponding channels of the A-group.

Horizontal Mach number gradients along the channel centerline and two walls for this family are shown in Figures 20-22. Here, again, the gradients along the centerline are somewhat less severe than those at the walls. Along the test section centerline the velocity deviations from the mean values range from 1.3 to 3.0%, whereas at the walls the deviations are from 2.1 to 4.6%.

Vertical Mach number gradients for the B-group of channels are measured at stations 5, 11.8 and 23.1 inches downstream of the point where the upper wall becomes straight and parallel to the lower. The distance between stations is 0.7 the test section height. These gradients are shown in Figures 23-25 for the three mean exit Mach numbers. The gradient trends at the three stations correspond to those obtained from the channels of the A-group for decreasing exit Mach numbers from 0.2 above to 0.5 below the design values. Inspection of Figures 22 and 25 which show the horizontal and vertical Mach number gradients for the B-4 channel reveals the presence of excessively large gradients. The reason for this is that the compression waves originating at the upper wall toward the end of the curved part are stronger than any previously encountered, owing to the large change in mean velocity from the high design value, and converge as they approach the lower wall. Their combined effect is like that of an oblique shock wave across which velocity

and flow inclination gradients are necessarily large. The method of characteristics no longer applies for constructing the flow accurately across regions where the gradients are so large because of the large changes in entropy. Recourse, then, must be had to the shock polar. Nevertheless, the method does indicate the presence of large gradients and in this investigation it is sufficient to be aware of them.

It should be noted that since the channel walls are parallel in the test section no mechanism exists for straightening out the flow and eliminating velocity gradients. Thus, no matter how far downstream the investigation might be carried out, the gradients will persist and the deviations of velocity and flow inclination from the mean values will undoubtedly be periodic with distance downstream.

B. Elimination of Gradients

In each of the channels of both groups that is investigated the fact that the flow is comparatively uniform in the test section suggests that the upper wall already is very close to the shape necessary to achieve absolutely uniform exit flow. This may be thought of in the following manner. The large changes in mean exit Mach number are effected by the sliding of one wall as described previously in order to alter the exit to throat height ratio. The non-uniformity of flow which then exists in the test section constitutes the perturbations on the mean flow caused by the deviation of the actual upper wall profile from the profile required for complete cancellation of all expansion waves impinging on it. Now, if the deviations between the actual and

required profiles are small as is expected, then conceivably, a supersonic wind tunnel employing the sliding wall principle could be operated over a wide range of uniform exit velocities by making the upper wall flexible between the throat and test section. New adjustment for Mach number in the test section would then consist of (1) sliding the lower wall and (2) making small changes in the upper wall shape. For each exit Mach number the upper wall can be altered the proper amount by a few strategically located mechanical jacks. To verify this contention the channel A-6 of the first group is constructed. The upper wall in the vicinity of the throat is kept the same but is redesigned downstream of the point where cancellation of expansion waves from the lower wall is desired. The selection of that particular point is governed by only two considerations: (1) the throat height and (2) the desired exit Mach number. In actual wind tunnel design since it is desirable to keep the height of the test section constant for all exit velocities then for an asymmetric channel of fixed exit or test section height a unique relationship exists between the throat height (or the exit velocity) and the location of the point on the upper wall at which wave cancellation is begun. In the design of the A-6 channel the position of the point beyond which the upper wall is redesigned is estimated on the basis of the throat height selected and the exit velocity necessary to give the same test section height. On the channel drawings B-2, B-4, and B-5 are superimposed the profiles of the upper wall necessary to effect a cancellation of all waves impinging thereon. In these cases the wall in the vicinity

of the throat as well as the throat height are unaltered with the design of the upper wall commencing at the point estimated from considerations mentioned above. The redesigned walls give, in every case, a test section height differing from the original by 0.0 to 2.5% owing to the errors made in estimating the position of the points where wave cancellation is begun. Another reason for the discrepancies is due to the method of characteristics itself; this is explained on p. 30 above. In the cases of B-2 and B-4 the redesigned walls result in test section heights practically the same as that of the original channel configuration, B-1. The maximum upper wall ordinate deviations occurring between the throat and test section are 1.5% and 0.6% respectively.

VI. CONCLUSIONS

On the basis of the flow field solutions carried out by the method of characteristics both for the Ringleb channel and the arbitrary two-dimensional asymmetric channels the following conclusions may be drawn.

1. In a channel having an exit Mach number of about 2 a net of characteristics which has a flow inclination increment between adjacent initial points on the initial line of 0.6° will give a maximum deviation of velocity from the theoretical value of the order 1% and a root-mean-square velocity deviation along the two boundaries from throat to exit of the order 0.5%. A net having twice this flow inclination increment between initial points may give a maximum deviation of velocity as high as 3% and a root-mean-square velocity deviation of the order 1%.
2. Errors in the magnitude of velocity and distribution of flow inclination along the initial line, from which the solution of the flow by the characteristics method is carried out, tend to decrease downstream. Some idea of this decrease is afforded by the flow between two Ringleb streamlines, C-3. Errors in velocity and flow inclination at the extremities of the initial line of about $\pm 2\%$ and 0.2° to 1.0° are present. In the downstream half of the channel the maximum error in velocity along the boundaries is 0.6%, the root-mean-square error is 0.3%, and maximum

error in flow inclination is 0.3°.

3. In the particular channel shapes chosen, if one wall is moved relative to the other in the direction of the exit flow a non-uniform flow field results in the test section. The deviations from the mean velocity are larger at the walls than at the channel centerline and are greatest for the largest change in mean exit velocity from the design value. The A-group of channels gives maximum deviations of velocity and flow inclination along the channel centerline of 0.8 to 1.2% and $\pm 0.8^{\circ}$, whereas the B-group gives maximum deviations of 1.3 to 3.0% and 1.5° to -1.2° along the centerline respectively.

4. A supersonic wind tunnel utilizing the principle of a sliding wall can be operated free of gradients in the test section over a wide range of velocities in the test section by altering the shape of the upper wall slightly. The maximum change required in the ordinates of the upper wall of channel B-2 is about 1.5% in order to give an exit Mach number 0.2 above the design value. The corresponding maximum change required in channel B-4 for which the exit Mach number is 0.2 below the design value is about 0.6%.

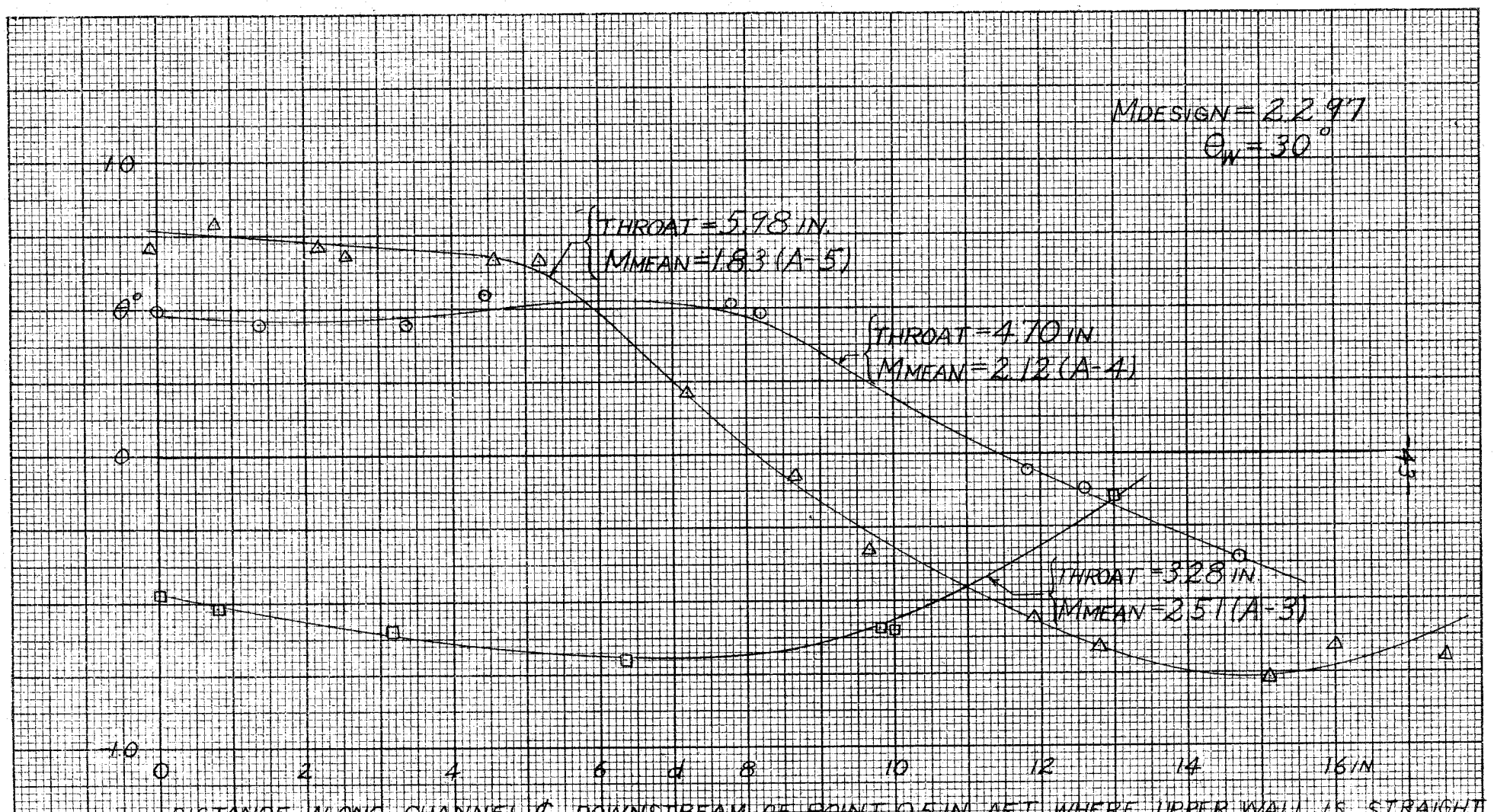

HORIZONTAL FLOW INCLINATION GRADIENTS

FIG. 12

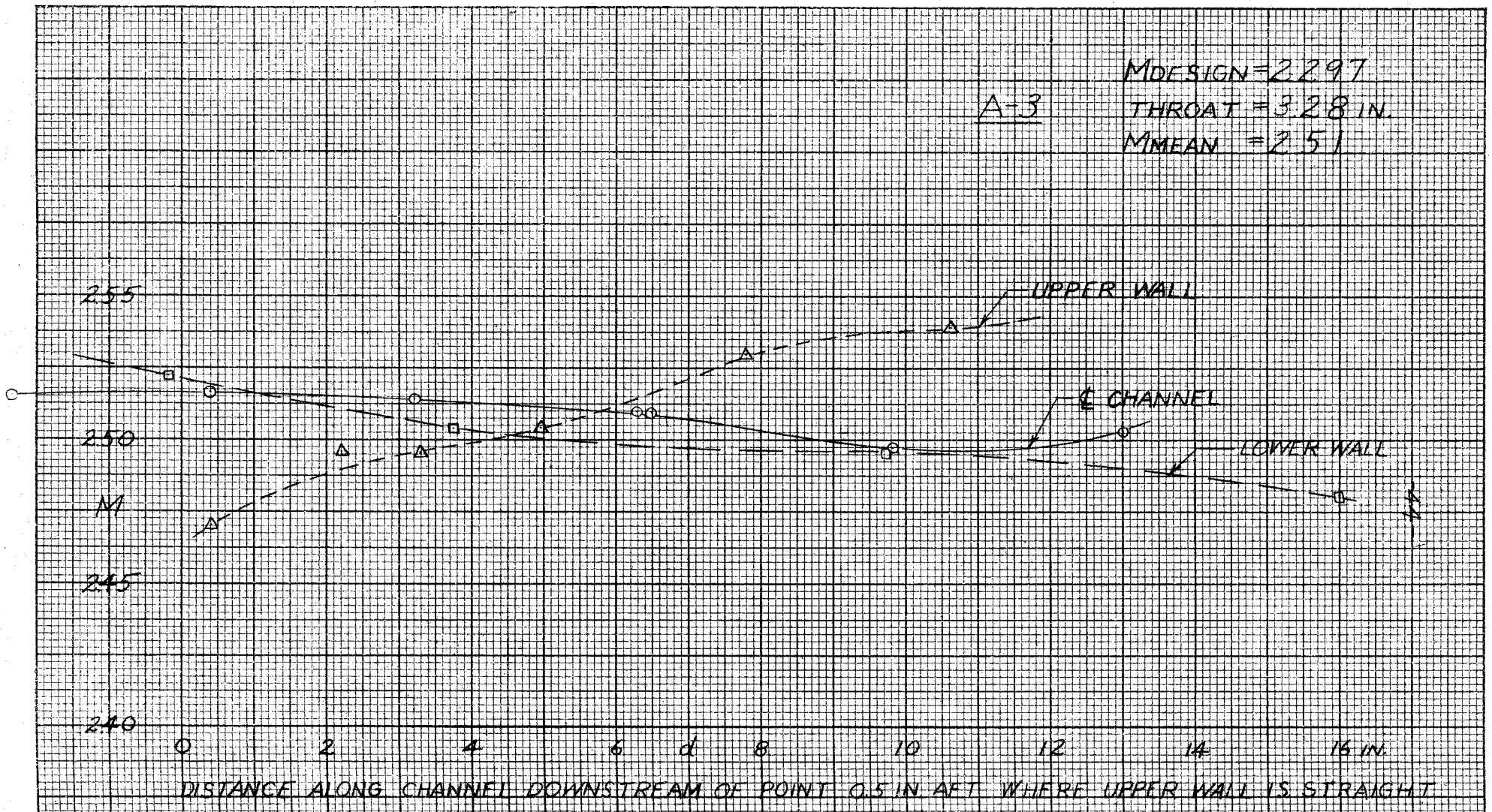

HORIZONTAL VELOCITY GRADIENTS

FIG 13

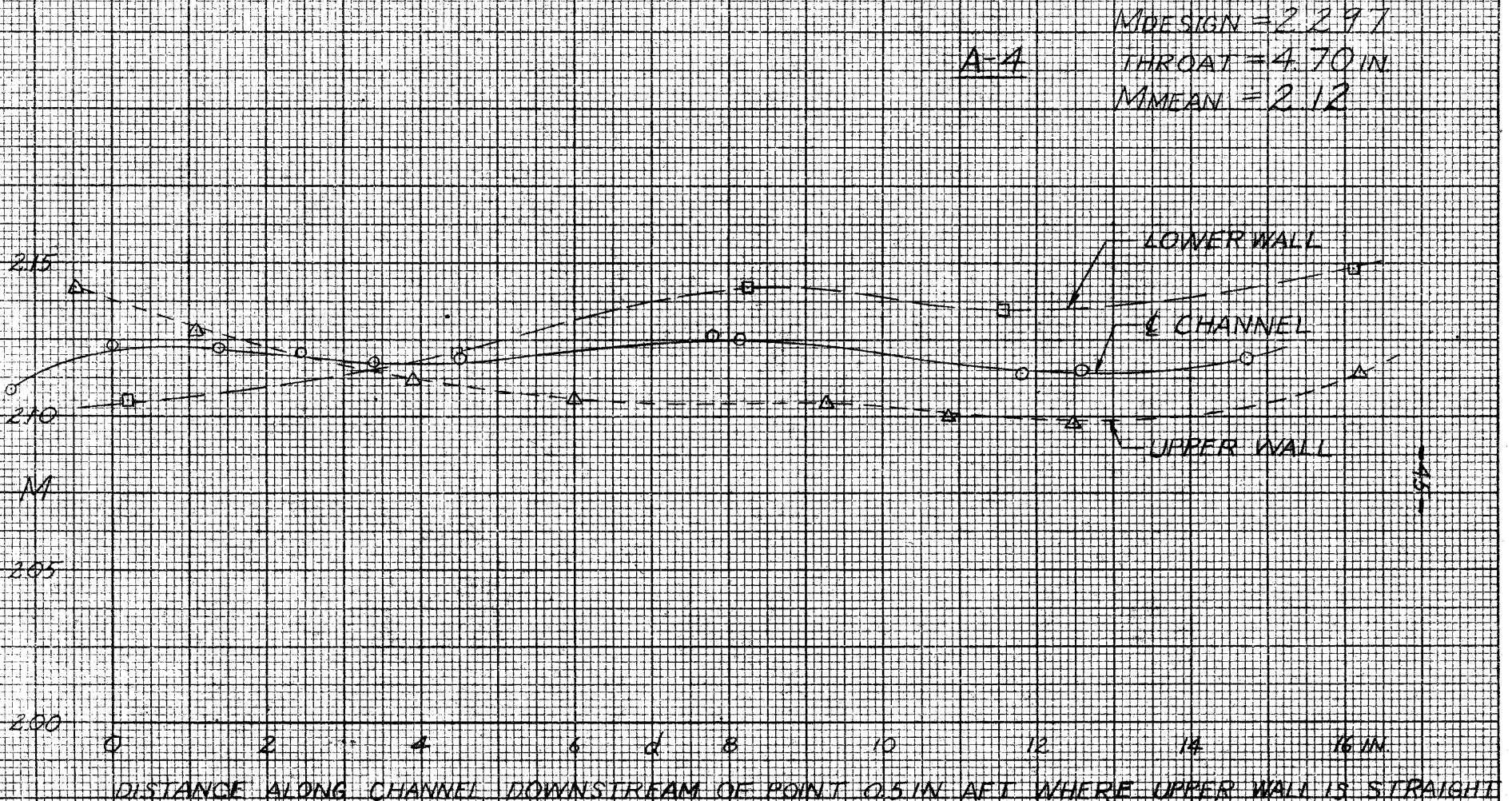

HORIZONTAL VELOCITY GRADIENTS

FIG 14

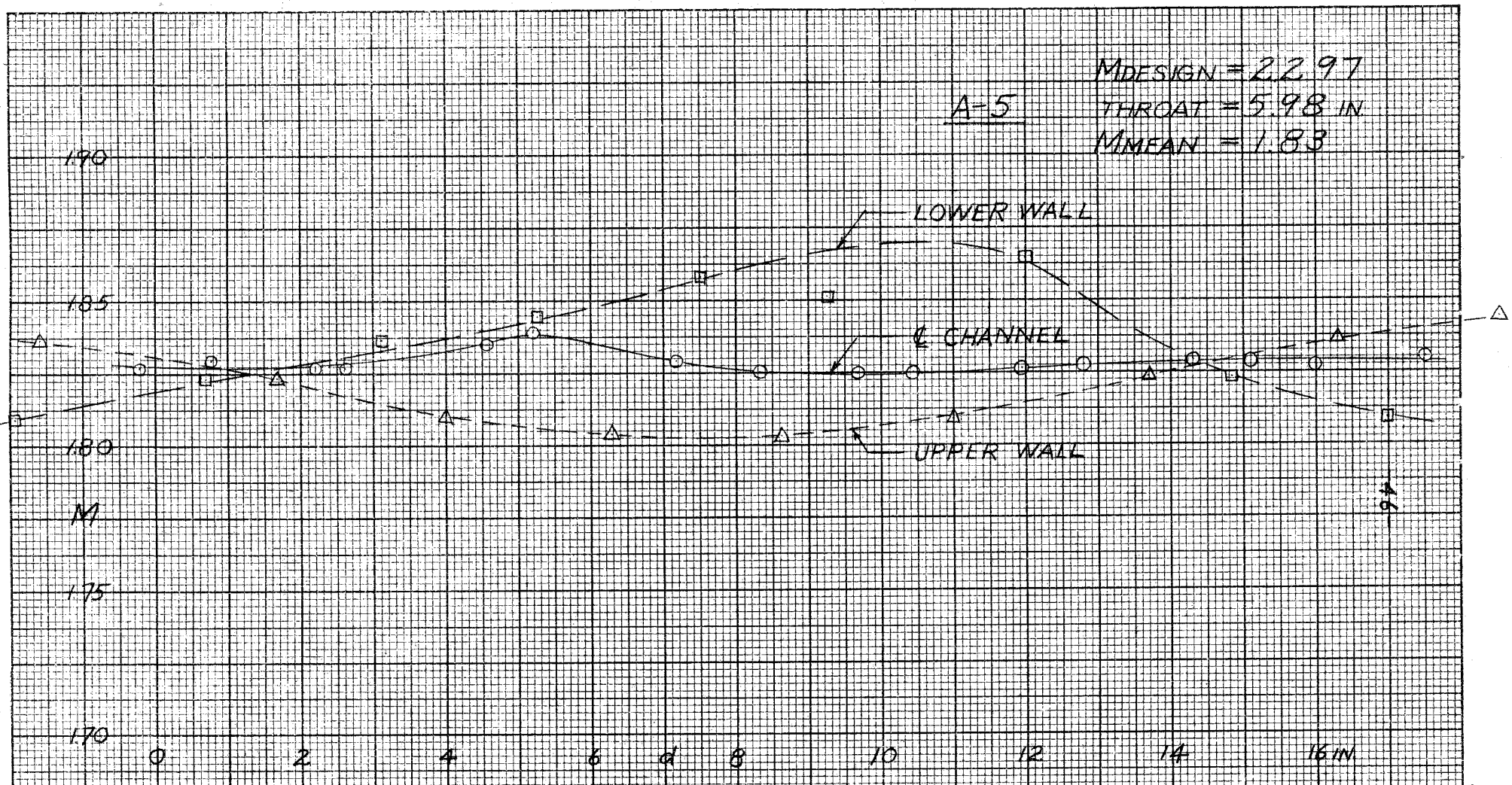

HORIZONTAL VELOCITY GRADIENTS

FIG 15

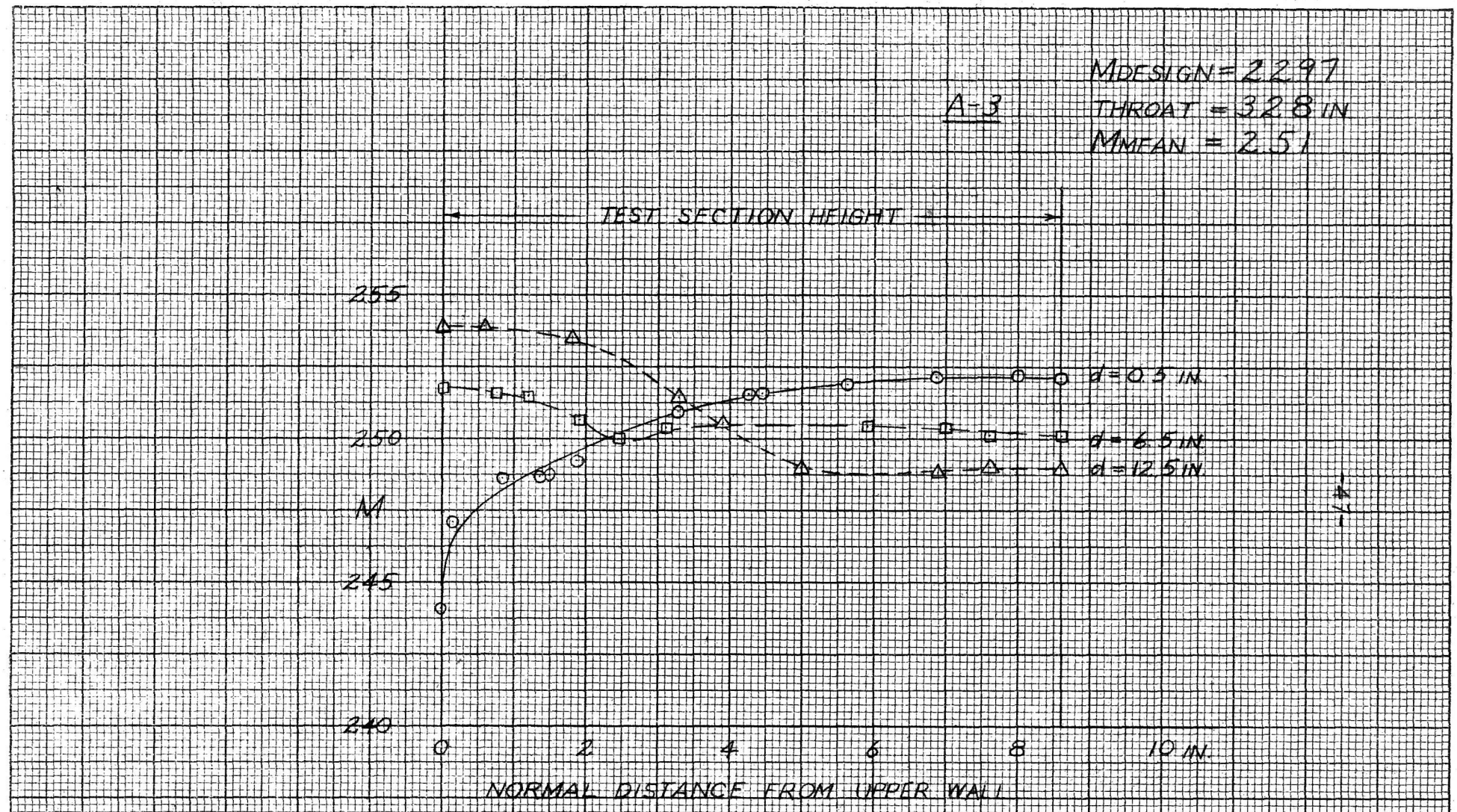

VERTICAL VELOCITY GRADIENTS

FIG 16

$M_{DESIGN} = 2.297$

A-4 $THROAT = 4.70$ IN

$M_{MEAN} = 2.12$

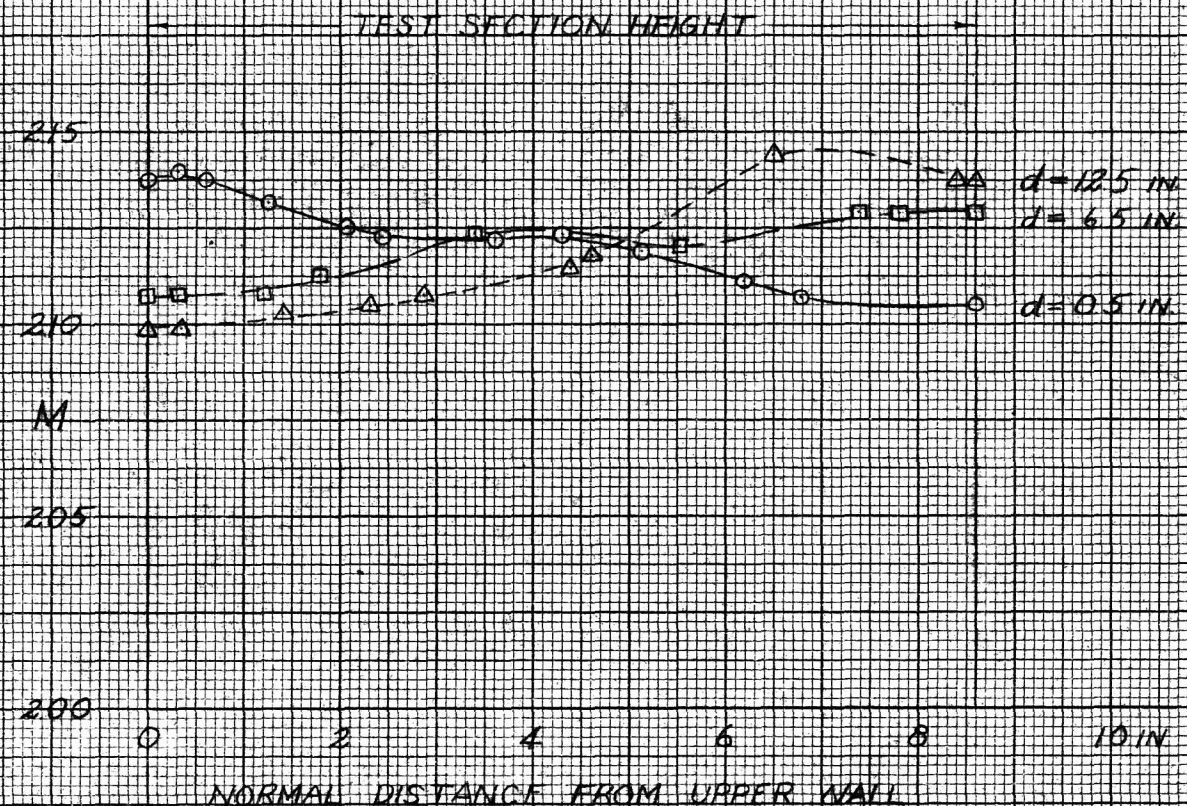

VERTICAL VELOCITY GRADIENTS

FIG 17

A-5

$M_{DESIGN} = 2.297$

THROAT $= 5.98$

$M_{MEAN} = 1.83$

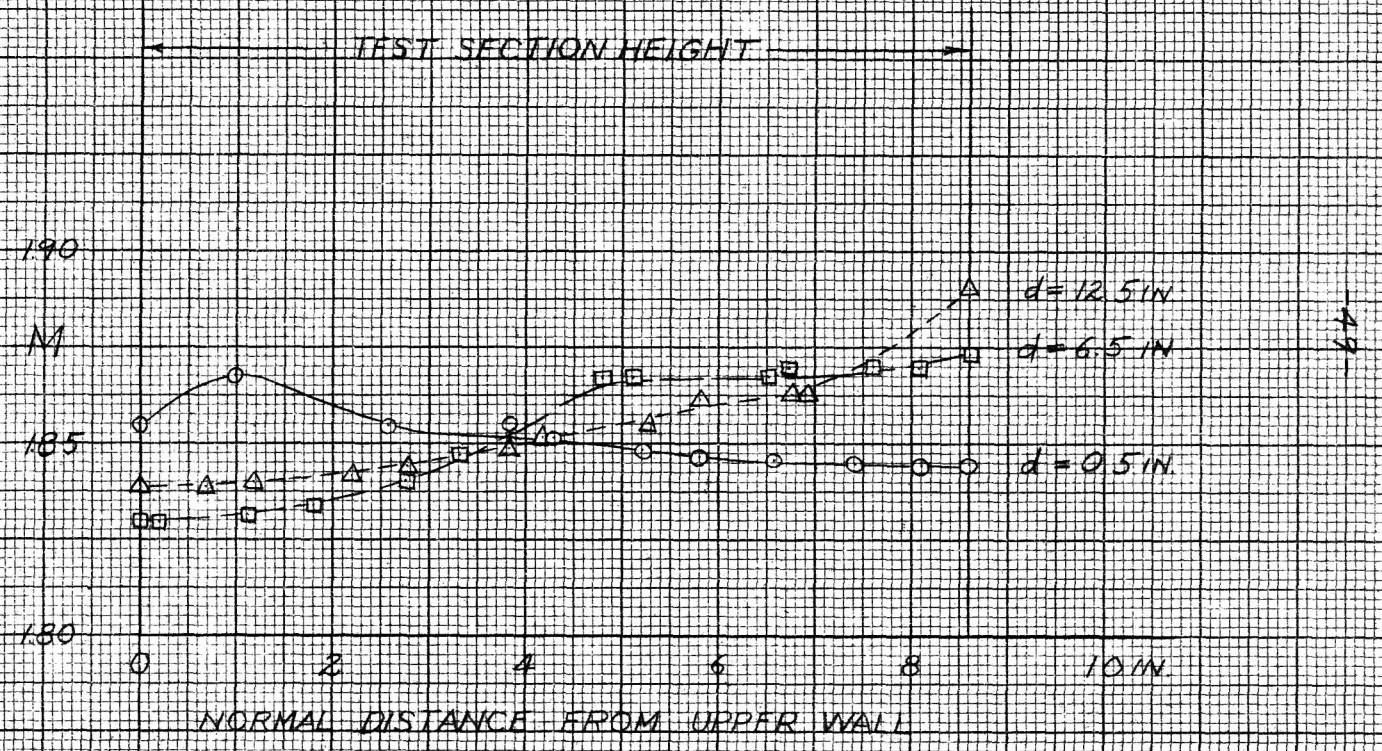

VERTICAL VELOCITY GRADIENTS

FIG 18

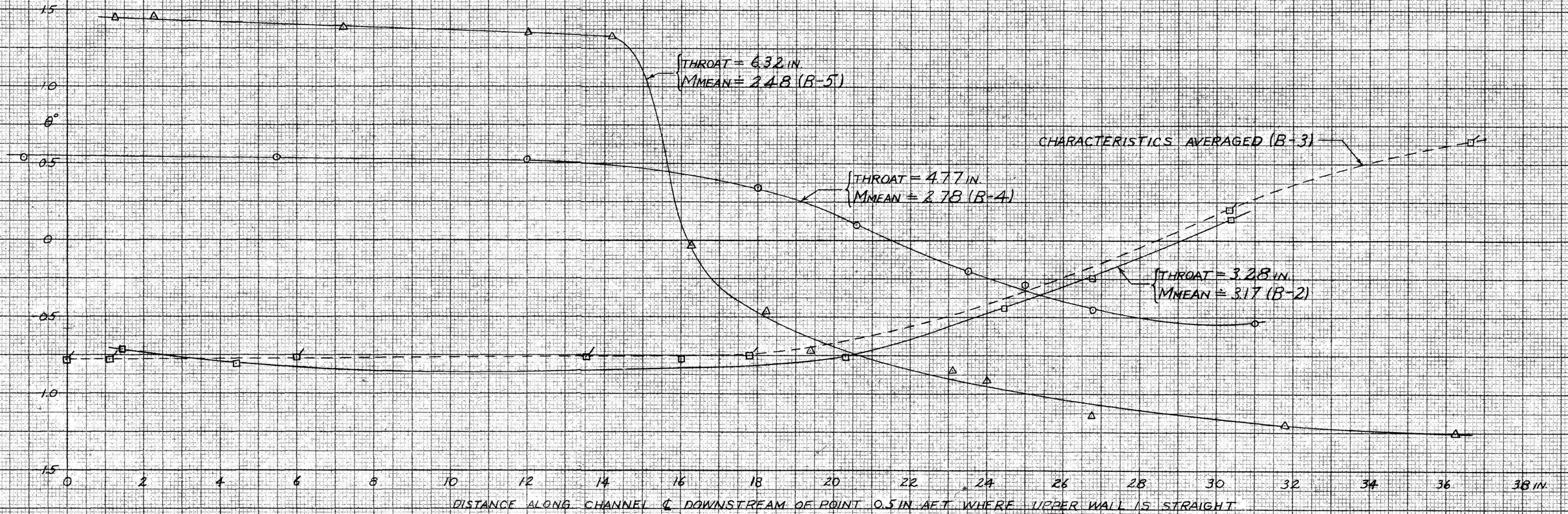

HORIZONTAL FLOW INCLINATION GRADIENTS

FIG. 19

FIG. 19

B-2

$M_{DESIGN} = 2.973$
THROAT = 32.8 IN.
$M_{MEAN} \doteq 3.17$

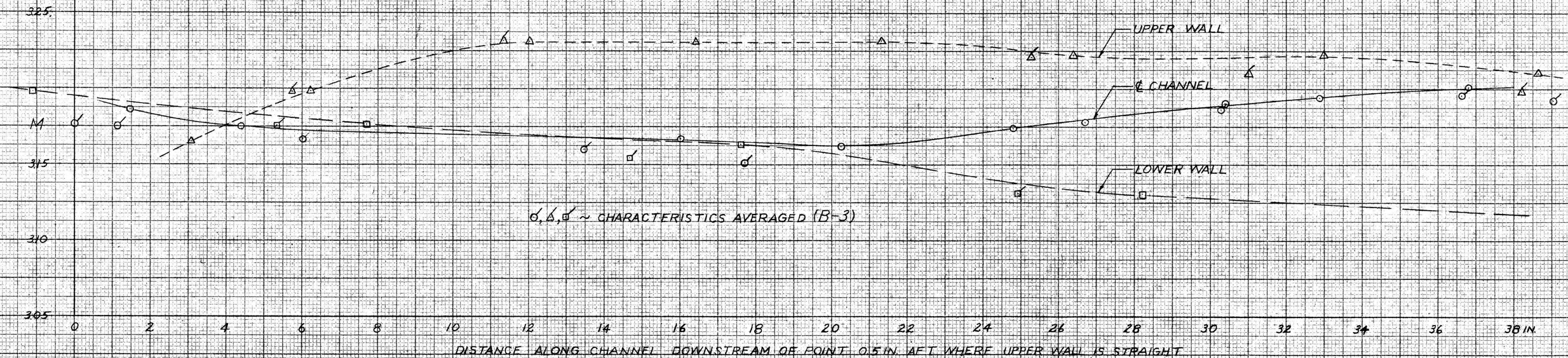

σ, Δ, ▫ ~ CHARACTERISTICS AVERAGED (B-3)

DISTANCE ALONG CHANNEL DOWNSTREAM OF POINT 0.5 IN. AFT WHERE UPPER WALL IS STRAIGHT

HORIZONTAL VELOCITY GRADIENTS

FIG. 20

FIG. 20

B-4

$M_{DESIGN} = 2.973$
THROAT = 4.77 IN.
$M_{MEAN} = 2.78$

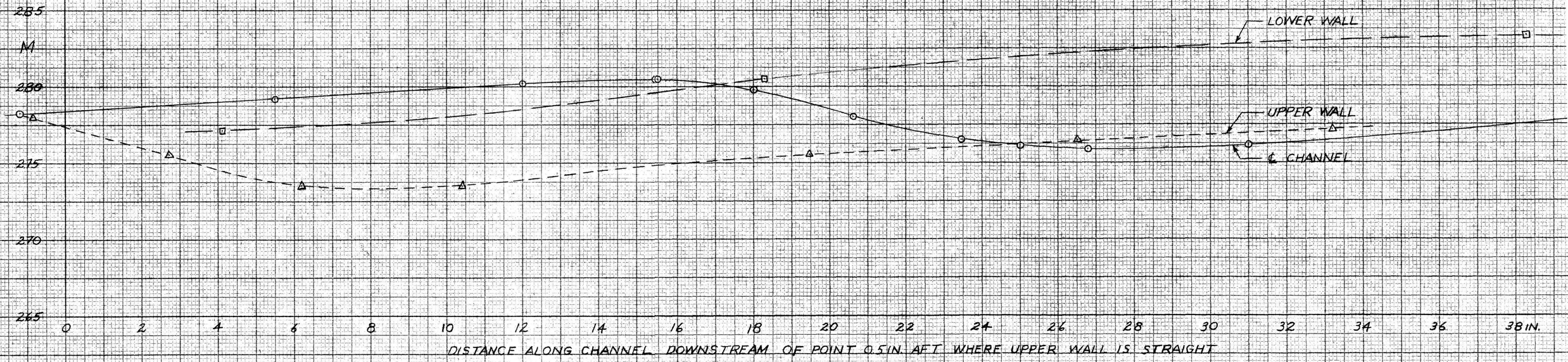

HORIZONTAL VELOCITY GRADIENTS

FIG 21

FIG. 21

B-5

$M_{DESIGN} = 2.973$
THROAT = 6.32 IN.
$M_{MEAN} = 2.48$

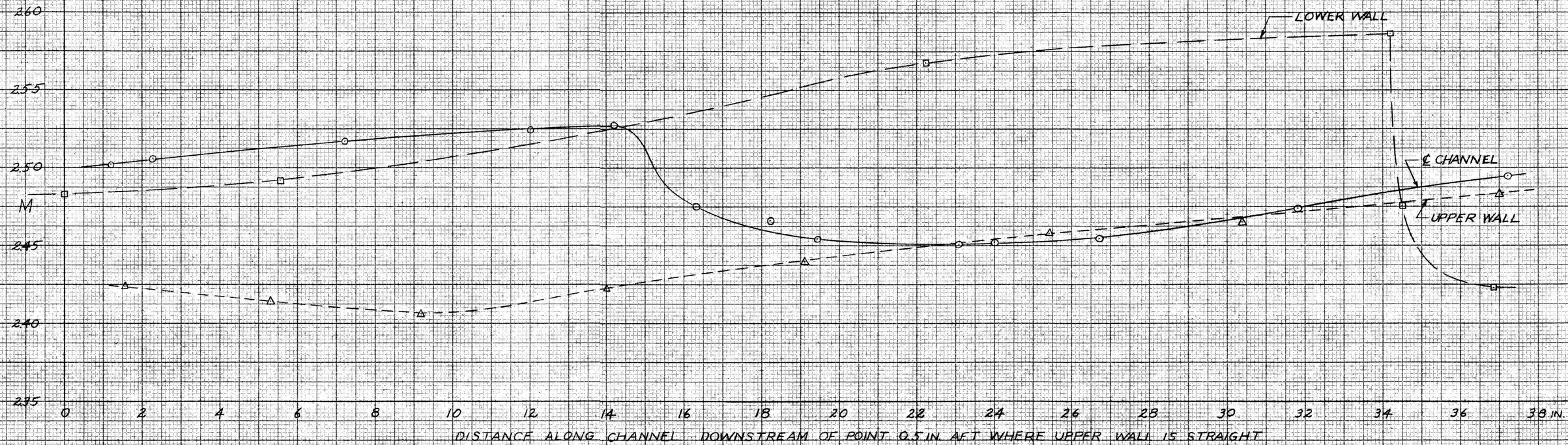

HORIZONTAL VELOCITY GRADIENTS

FIG 22

FIG 22

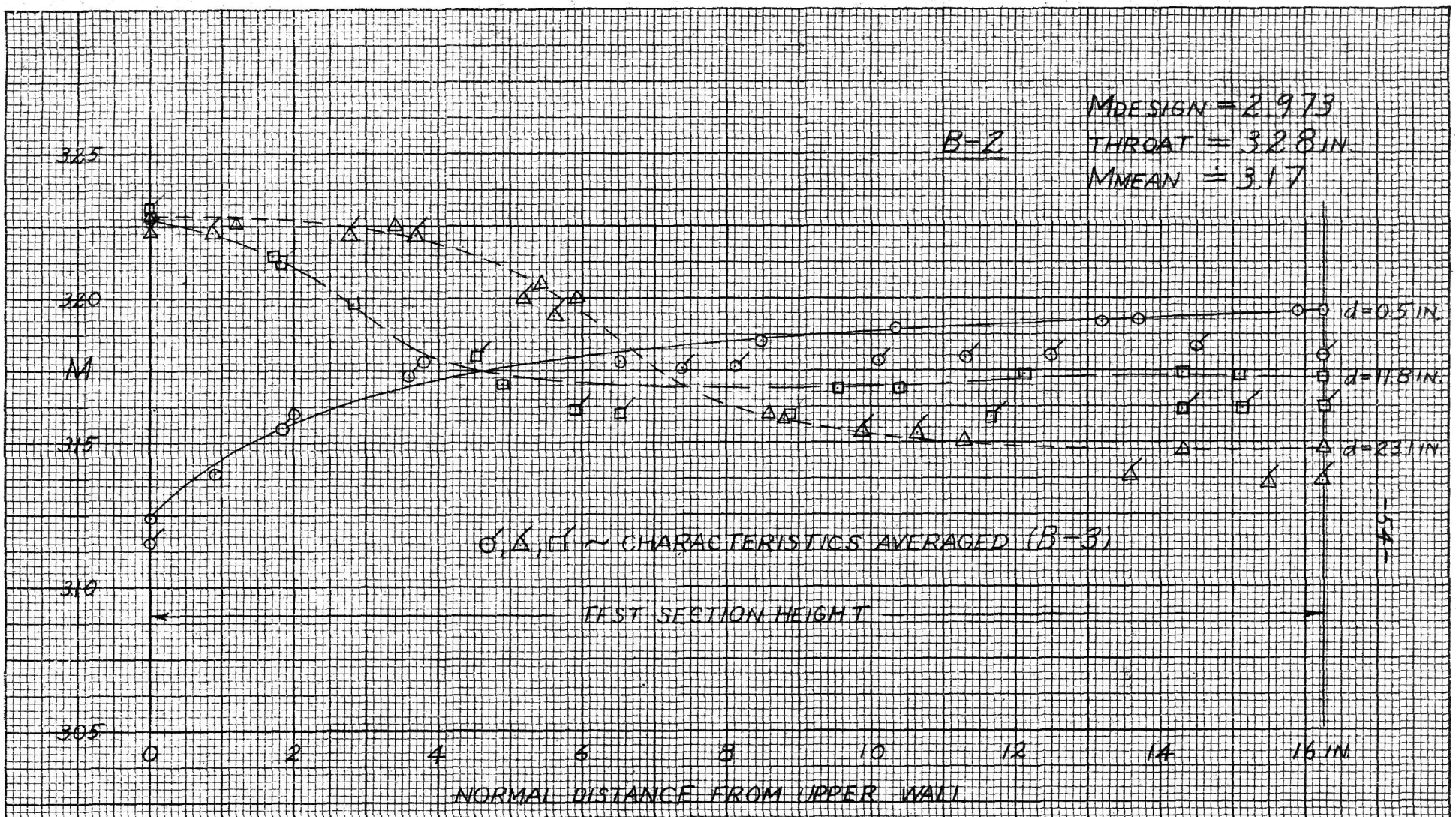

VERTICAL VELOCITY GRADIENTS

FIG 2.3

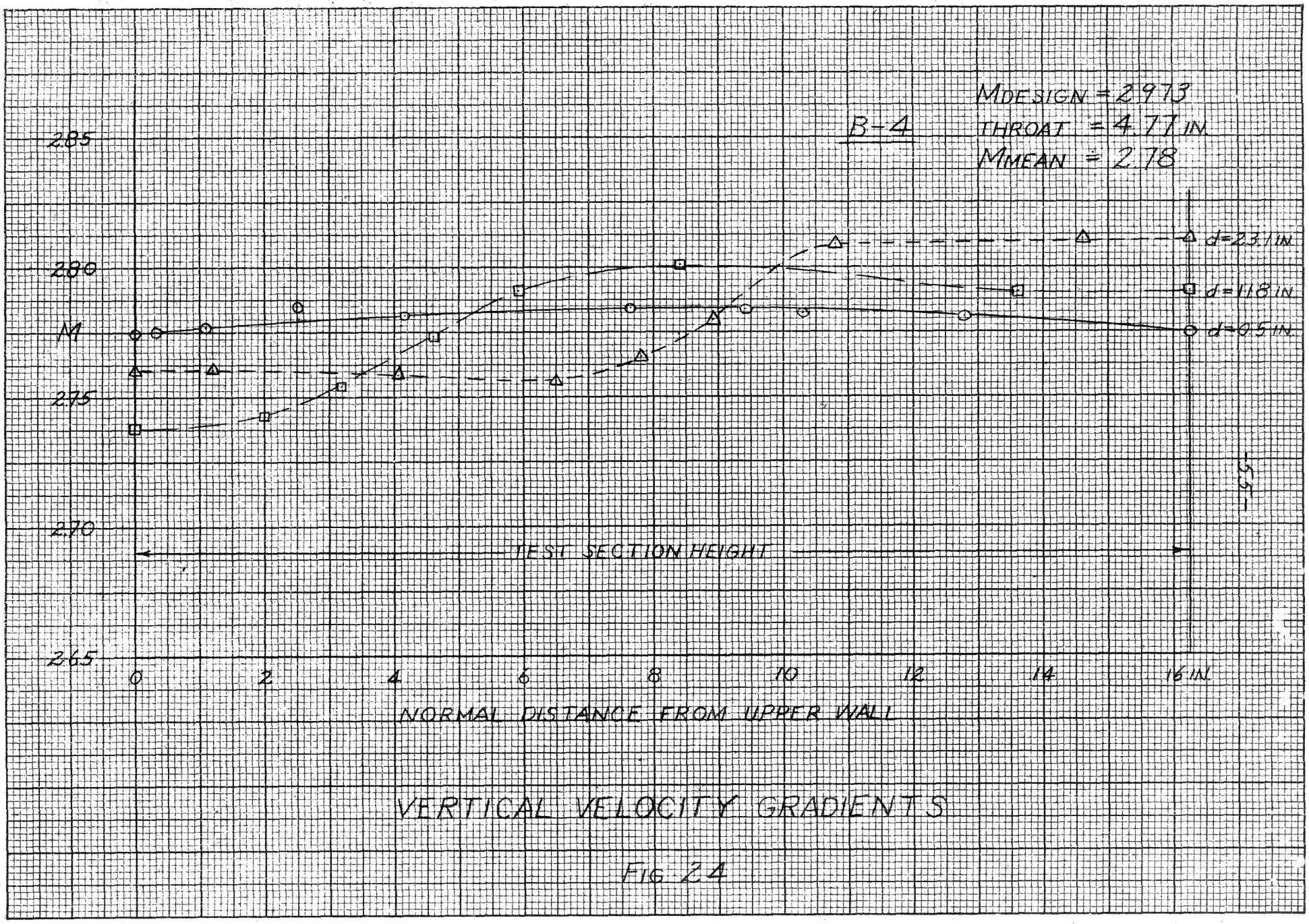

VERTICAL VELOCITY GRADIENTS

FIG 24

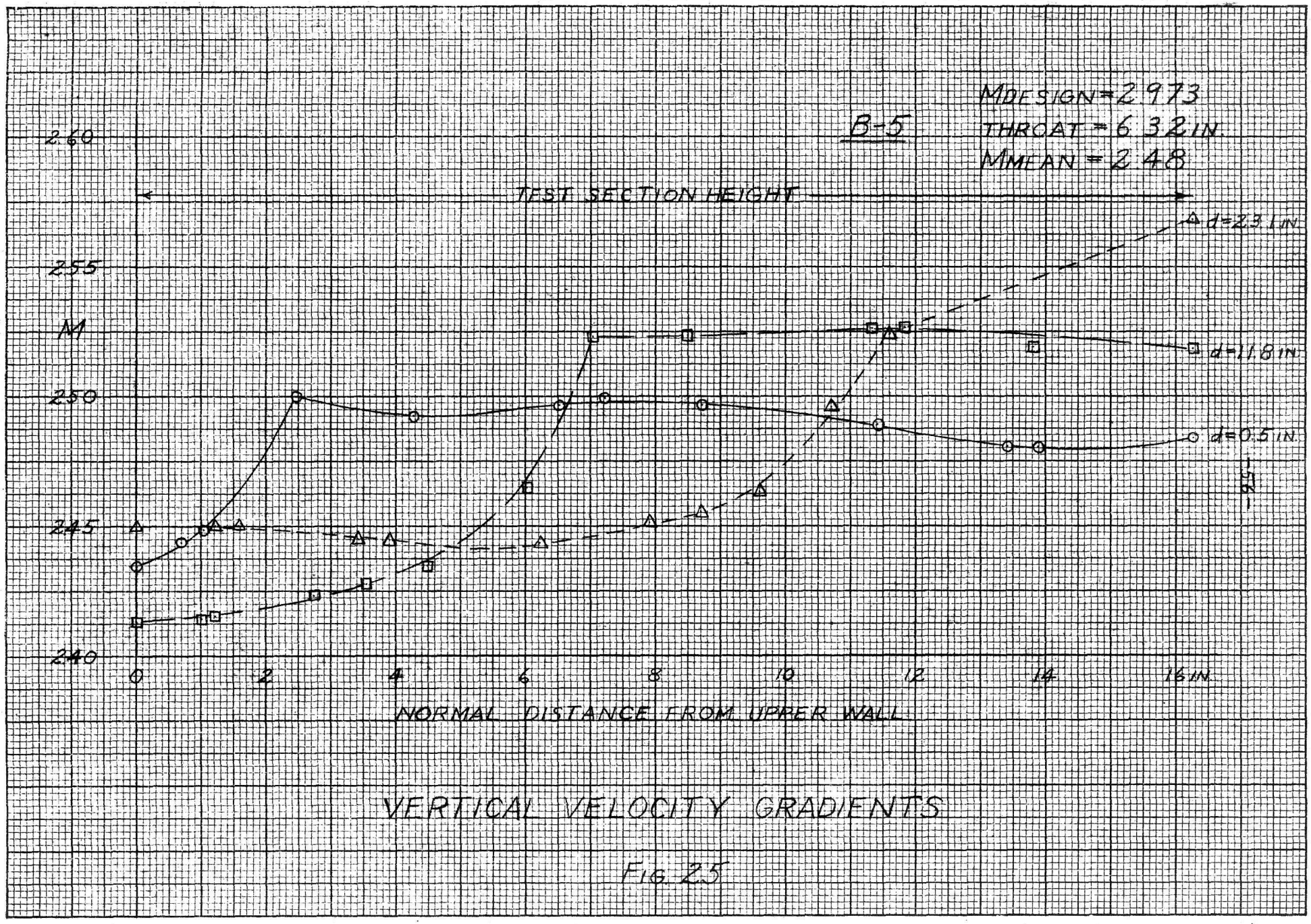

VERTICAL VELOCITY GRADIENTS

FIG. 25

A-3 $M_{DESIGN} = 2.297$, THROAT = 3.28 IN, $M_{MEAN} = 2.51$

NOTE
1. AT EACH LATTICE POINT THE UPPER NUMBER IS THE ANGLE OF FLOW INCLINATION AND THE LOWER NUMBER IS THE PRANDTL-MEYER ANGLE IN DEGREES AT THE POINT.
2. DASHED LINES INDICATE WAVES OF ZERO STRENGTH.
3. WALL INCLINATIONS ARE NOTED ALONG THE TWO WALLS.

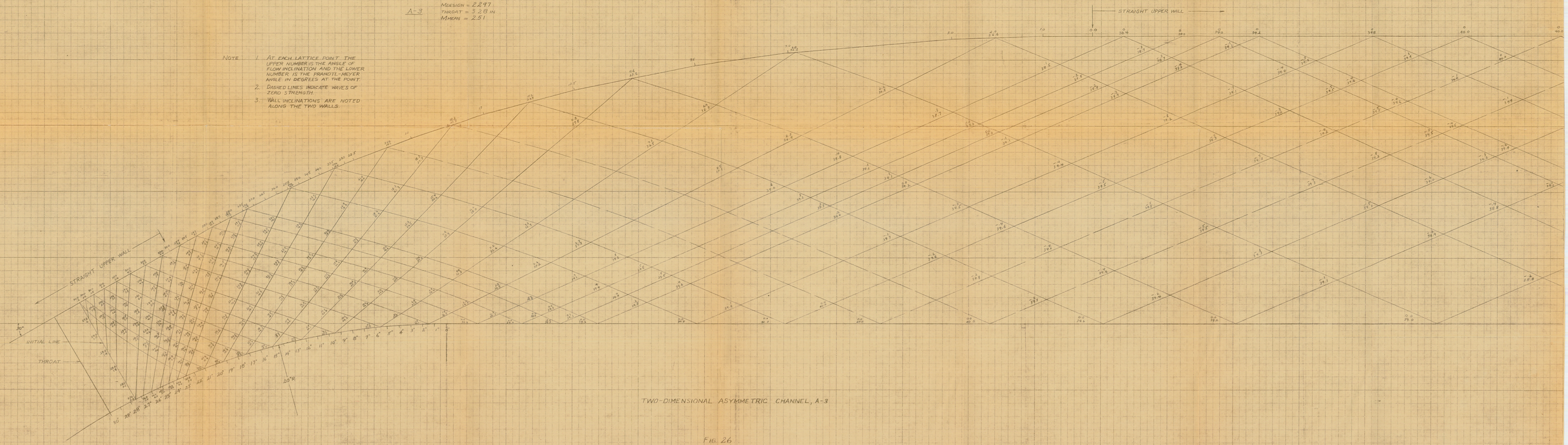

TWO-DIMENSIONAL ASYMMETRIC CHANNEL, A-3

FIG. 26

REFERENCES

1. "Exakte Lösungen der Differentialgleichungen einer adiabatischen Gasströmung", by F. Ringleb; ZAMM, August 1940, pp. 185-198.

2. "General Characteristics of the Flow Through Nozzles at Near Critical Speeds", by R. Sauer; N.A.C.A. T.M. No. 1147, June 1947.

3. "Näherungsverfahren zur zeichnerische Ermittlung von ebenen Strömmungen mit Überachall geschwindigkeit", by L. Prandtl and A. Busemann; Stodola Festschrift, Zurich, 1929, pp. 499-509.

4. "Numerical-Graphical Methods of Characteristics for Plane Potential Shock-Free Flow Problems", by L. L. Cronvich; Journal of the Aeronautical Sciences, Vol. 14, No. 4, April 1947, pp. 237-242.

5. "Flow Angle - Mach Number - Area Ratio Table for Supersonic Nozzle Design", Guggenheim Aeronautical Laboratory, California Institute of Technology.

APPENDIX

Pro-Rating of Flow Inclinations Along Initial Line

The following method of pro-rating flow inclinations along the initial line is adopted for C-3 and the channels in the A and B groups. The channel A-3 is taken as an illustration.

The position of the initial line is first determined. Referring to Fig. 1-a we have for dimensions at the throat

$$y_s = 3.28'', \quad R_1 = 20'',$$

$$\frac{R_1}{y_s} = \frac{20}{3.28} = 6.10 .$$

Using equation (5) in which ρ_s is the same as R_1 we obtain

$$\alpha = .0797.$$

Now, since the upper wall is straight in this region, equations (4) are applicable, and when $y=0$ we have

$$u = \alpha x .$$

Since it is desired to construct the initial line from the upper wall at the point where M = 1.050

$$x_D = \frac{u_{M=1.050}}{\alpha} = \frac{0.041}{0.0797} = 0.515''.$$

Equation (17a) of Ref. 2 gives the following expression for ϵ

$$\epsilon = \frac{\gamma+1}{6} \alpha y_s^2 ,$$

whence

$$\epsilon = 0.343'' .$$

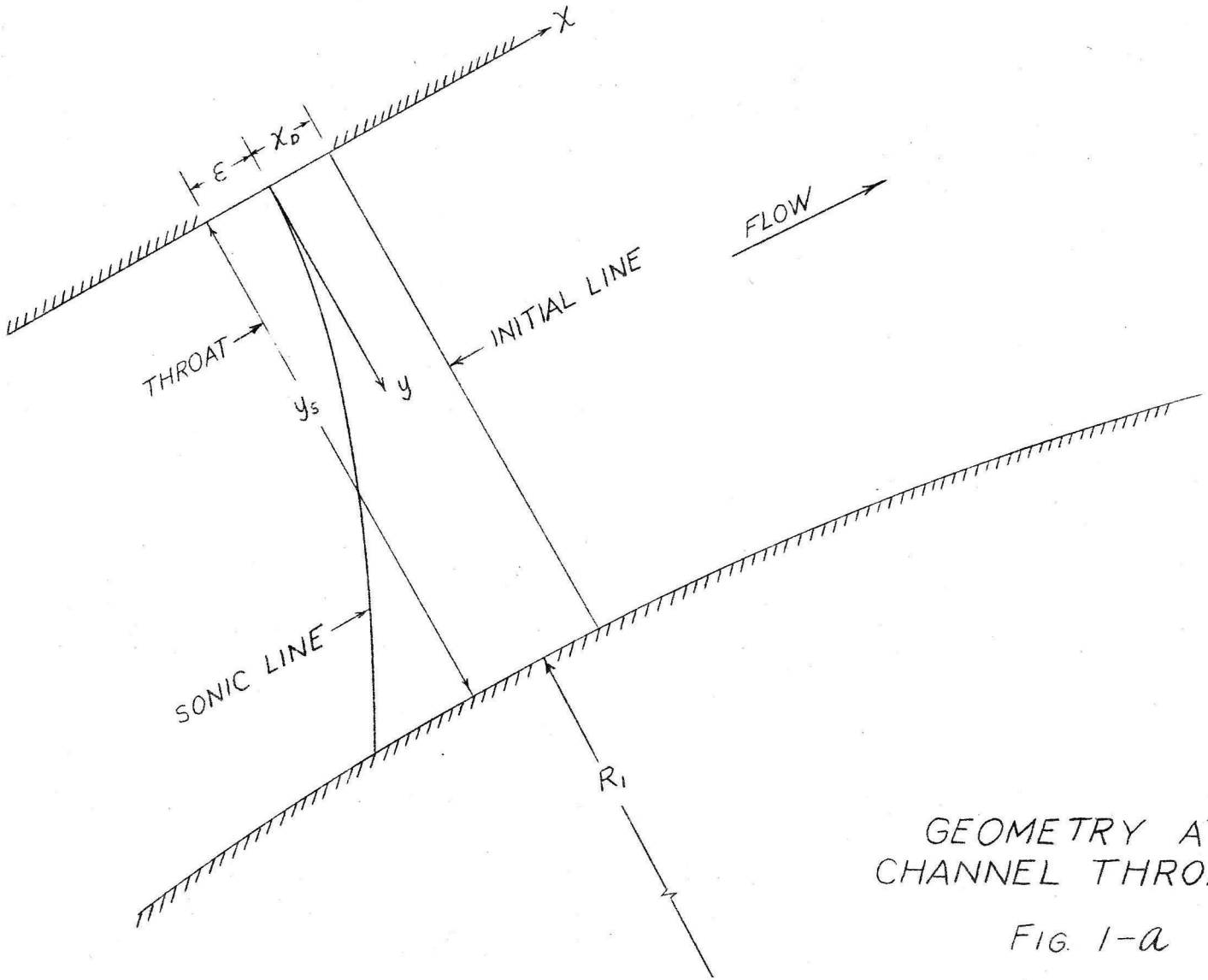

GEOMETRY AT
CHANNEL THROAT

FIG. 1-a

The initial line is constructed from a point on the upper wall at a distance $x_D + \epsilon = 0.858''$ downstream of the throat and, for convenience, parallel to the y axis. The initial line, DC, is then divided into 6 equal intervals. Each point, starting from the one on the lower wall, is assigned a number from 0 to 6 consecutively. Equations (4) applied to line DC reduce to

$$u = 0.041 + 0.00763y^2$$

$$v = 0.00785y + 0.000419y^3.$$

The following values are obtained at the points 0 to 6:

Pt.	u	v	$\frac{\tilde{w}}{a^*}$	M	$\tan\theta' = \frac{v}{1+u}$	θ'	θ
6	0.0410	0	1.041	1.050	0	0.00°	30.0°
5	.0433	0.0044	1.043	1.054	0.00419	.24	29.7
4	.0502	.0091	1.050	1.061	.00870	.50	29.4
3	.0615	.0147	1.062	1.076	.01387	.80	29.0
2	.0775	.0214	1.078	1.096	.01988	1.14	28.6
1	.0980	.0299	1.098	1.121	.02722	1.56	28.1
0	.1231	.0406	1.124	1.155	.03615	2.07	27.5

The values of θ' are the flow inclinations predicted by equations (4) where θ' is measured relative to the x axis, positive for clockwise angles. The true angle of flow, θ, relative to the direction of the walls at the exit is known at points 0 and 6 from the geometry of the channel. The values of θ assigned to the points 1 to 5 are obtained by subtracting from 30° the ratio of θ' at the point in question to the

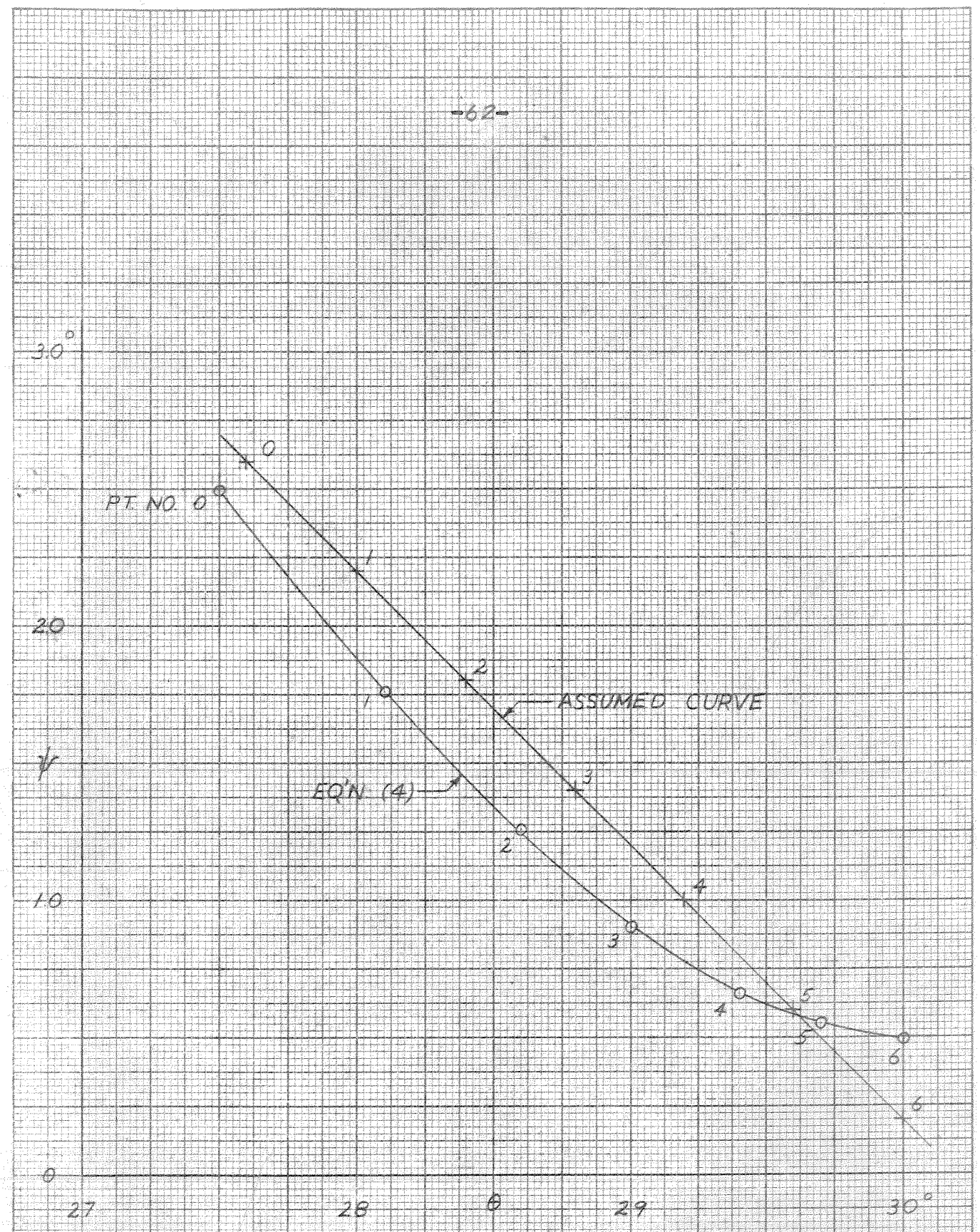

VARIATION OF PRANDTL-MEYER ANGLE WITH FLOW INCLINATION ALONG INITIAL LINE OF CHANNEL A-3

FIG. 2-a

difference in Θ' between points 0 and 6 which ratio is multiplied by the difference in Θ between points 0 and 6. For example, at point 4 we have

$$\Theta = 30^\circ - \frac{0.50}{2.07}(30^\circ - 27.5^\circ)$$

$$= 29.4^\circ$$

Method of Design of Upper Wall of An Asymmetric Channel by The Lattice-Point Method

Given the lower wall and the throat portion of the upper wall of an asymmetric channel, it is desired to construct the upper wall so that uniform flow at Mach number M_e obtains at the exit.

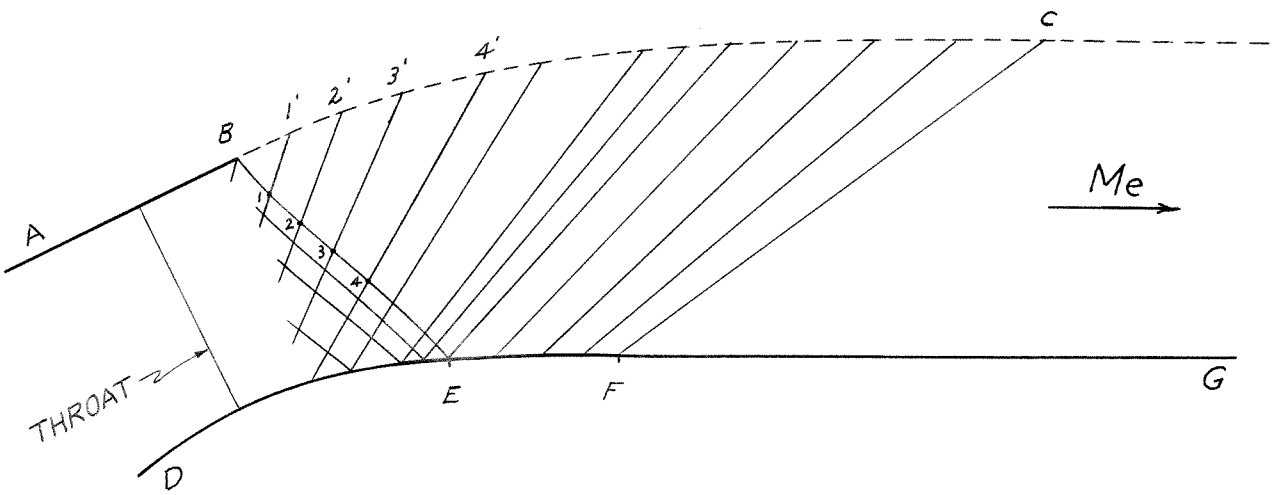

Fig. 3-a. Design of the Upper Wall of an Asymmetric Channel for Uniform Exit Velocity

In reference to Fig. 3-a above we have the lower wall DEFG and the portion of the upper wall AB given where AB need not be straight. At point F the inclination of the lower wall is the same as that of the uniform exit flow.

The flow field is constructed in the throat region by the methods described or by some other satisfactory method. Suppose that at point B the quantity $\theta+\psi$ is equal (or very nearly so) to ψ_e, the Prandtl-Meyer angle associated with M_e. Then all waves impinging upon the upper wall

beyond point B must be cancelled. The characteristic from the upper family is constructed from B terminating on the lower wall at, say, E. Now, the necessary condition that the wave of the lower family from point 1 be cancelled at the wall is that the values of ψ and θ at point 1' where it strikes the wall be the same as those at point 1. Likewise, the same condition holds for points 2' and 2, 3' and 3, etc. Because $\theta + \psi$ is equal to ψ_e along the characteristic BE and no expansion or compression waves originate at the upper wall beyond B, it follows that $\theta + \psi$ is equal to ψ_e along the lower wall beyond E and all characteristics of the lower family beyond BE are straight. Between points E and F expansion waves will emanate so that this portion of the wall may be subdivided into as many intervals as desired and straight characteristics of the lower family drawn from the division points. Point 1' on the upper wall is located by drawing a line from B at the average value of θ between points B and 1. Similarly point 2' is located by drawing a line from 1' at the average value of θ between points 1 and 2. The points B, 1', 2', 3' etc. represent closely the vertices of a polygon inscribed in the upper wall profile. If the basic net of characteristics is finer a greater number of the vertices may be located. The flow in the region EBCF is "lost solution" or Prandtl-Meyer flow; the flow beyond the characteristic FC is uniform at Mach number = M_e.